



Cisd2 plays an essential role in corneal epithelial regeneration

Chi-Chin Sun^{a,b}, Shao-Yun Lee^a, Cheng-Heng Kao^c, Li-Hsien Chen^d, Zhao-Qing Shen^e, Chia-Hui Lai^f, Tsai-Yu Tzeng^g, Jong-Hwei Su Pang^f, Wen-Tai Chiu^{h,*}, Ting-Fen Tsai^{e,i,j,k,**}

^a Department of Ophthalmology, Chang Gung Memorial Hospital, Keelung, Taiwan

^b School of Medicine, College of Medicine, Chang Gung University, Taoyuan, Taiwan

^c Center of General Education, Chang Gung University, Taoyuan, Taiwan

^d Department of Pharmacology, National Cheng Kung University Hospital, College of Medicine, National Cheng Kung University, Taiwan

^e Department of Life Sciences and Institute of Genome Sciences, National Yang Ming Chiao Tung University, Taipei, Taiwan

^f Graduate Institute of Clinical Medical Sciences, Chang Gung University, Kwei-shan, Taoyuan, Taiwan

^g Cancer Progression Research Center, National Yang Ming Chiao Tung University, Taipei, Taiwan

^h Department of Biomedical Engineering, College of Engineering, National Cheng Kung University, Tainan, Taiwan

ⁱ Aging and Health Research Center, National Yang Ming Chiao Tung University, Taipei, Taiwan

^j Institute of Molecular and Genomic Medicine, National Health Research Institutes, Zhunan, Taiwan

^k Institute of Biotechnology and Pharmaceutical Research, National Health Research Institutes, Zhunan, Taiwan

ARTICLE INFO

Article History:

Received 28 July 2021

Revised 24 September 2021

Accepted 14 October 2021

Available online xxx

Keywords:

corneal wound healing

Cisd2

calcium homeostasis

limbal stem cell deficiency

EDTA

cyclosporine A

ABSTRACT

Background: Age-related changes affecting the ocular surface cause vision loss in the elderly. Cisd2 deficiency drives premature aging in mice as well as resulting in various ocular surface abnormalities. Here we investigate the role of Cisd2 in corneal health and disease.

Methods: We studied the molecular mechanism underlying the ocular phenotypes brought about by Cisd2 deficiency using both Cisd2 knockout (KO) mice and a human corneal epithelial cell (HCEC) cell line carrying a CRISPR-mediated Cisd2KO background. We also develop a potential therapeutic strategy that targets the Ca²⁺ signaling pathway, which has been found to be dysregulated in the corneal epithelium of subjects with ocular surface disease in order to extend the mechanistic findings into a translational application.

Findings: Firstly, in patients with corneal epithelial disease, Cisd2 is down-regulated in their corneal epithelial cells. Secondly, using mouse cornea, Cisd2 deficiency causes a cycle of chronic injury and persistent repair resulting in exhaustion of the limbal progenitor cells. Thirdly, in human corneal epithelial cells, Cisd2 deficiency disrupts intracellular Ca²⁺ homeostasis, impairing mitochondrial function, thereby retarding corneal repair. Fourthly, cyclosporine A and EDTA facilitate corneal epithelial wound healing in Cisd2 knockout mice. Finally, cyclosporine A treatment restores corneal epithelial erosion in patients with dry eye disease, which affects the ocular surface.

Interpretation: These findings reveal that Cisd2 plays an essential role in the cornea and that Ca²⁺ signaling pathways are potential targets for developing therapeutics of corneal epithelial diseases.

Funding: This study was supported by the Ministry of Science and Technology (MOST) and Chang Gung Medical Research Foundation, Taiwan.

© 2021 The Authors. Published by Elsevier B.V. This is an open access article under the CC BY-NC-ND license (<http://creativecommons.org/licenses/by-nc-nd/4.0/>)

1. Introduction

The normal ocular surface consists of corneal, limbal, and conjunctival epithelial cells that, together with the pre-ocular tear film, maintain its integrity. Clarity of the cornea is a prerequisite for good visual

acuity and mainly relies on a dynamic equilibrium involving the proliferation of the basal epithelium, the centripetal migration of peripheral epithelium, and the shedding of epithelial cells into the tear pool. The whole process is traditionally recognized as the “X-Y-Z” hypothesis for corneal epithelial maintenance [1]. Disrupted corneal epithelial layers can lead to persistent corneal epithelial defects, which are manifested as chronic inflammation, neovascularization, ulceration, scarring, and even perforation of the cornea [2]. Several etiologies that result in corneal epithelial defects have been described, including dry eye, chemical burns, corneal limbal stem cell deficiency (LSCD), neurotrophic keratitis, and diabetes mellitus [3].

* Corresponding Authors. Wen-Tai Chiu, Ph.D., No. 1, University Rd., Tainan City 701, Taiwan

** Corresponding Authors. Ting-Fen Tsai, Ph.D., 155 Li-Nong St., Sec. 2, Beitou, Taipei 11221, Taiwan

E-mail addresses: wtchiu@mail.ncku.edu.tw (W.-T. Chiu), tftsai@ym.edu.tw (T.-F. Tsai).

Research in context

Evidence before this study

Persistent corneal epithelial defect (PCED) resulted from various etiologies is one of the global leading causes for blindness. Lack of effective treatment for recalcitrant PCED will inevitably lead to corneal scar, perforation and even loss of the eye. Previous study indicates that CDGSH iron-sulfur domain-containing protein 2 (Cisd2) deficiency, disturbing Ca^{2+} homeostasis, results in a variety of ocular surface abnormalities. However, the expression and the functional role of Cisd2 in the cornea has not been investigated.

Added value of this study

We, for the first time, find that Cisd2 is dramatically down-regulated in patients with corneal epithelial disease. Additionally, Cisd2 deficiency in mice leads to chronic corneal epithelial damage and impairs epithelial wound healing. Mechanistically in human corneal epithelial cells, Cisd2 deficiency hinders cell proliferation and migration via increasing basal cytosolic Ca^{2+} levels, impairing mitochondrial function and increasing oxidative stress. Furthermore, in Cisd2KO mice, CsA and EDTA are both able to facilitate epithelial wound healing of the cornea, improve corneal transmittance and suppress inflammatory responses. Finally, and remarkably, topical CsA treatment is able to restore corneal epithelial erosion in patients suffering from moderate to severe dry eye disease.

Implications of all the available evidence

This study reveals the translational significance of Cisd2 in corneal epithelial regeneration, and provides evidence that Ca^{2+} signaling pathways are potential targets for the development of therapeutics for corneal epithelial diseases in humans.

fully understood how Ca^{2+} dysregulation impairs epithelial wound healing in the cornea. Accordingly, an appropriate animal model is important to providing an experimental platform for understanding the molecular mechanism underlying the process of impaired wound healing that leads to corneal opacity. Currently there are two animal models available, these are acute chemical injury [14] and mechanical keratectomy [15]; both have been used to create corneal wounds for research investigations. However, an animal model, with precise modification of the specific genetic factors, is needed in order to carry out mechanistic investigations aimed at elucidating the molecular pathogenesis and intrinsic defective signaling pathways in the cornea and up to the present no such system has been described in the literature.

The CDGSH iron-sulfur domain-containing protein 2 (CISD2) has been identified as the causative gene for Wolfram syndrome 2 (WFS2) [16,17]. WFS is an autosomal recessive neurodegenerative disorder in humans that is primarily characterized by juvenile onset diabetes mellitus, optical atrophy and premature death [18]. In Cisd2 knockout (KO) mice, Cisd2 deficiency drives premature aging [19,20]. Intriguingly, Cisd2 deficiency also results in a variety of ocular surface abnormalities as evidenced by corneal opacity, corneal neovascularization and surface keratinization. These findings suggest that the genetic defect, namely when the absence of Cisd2, affects the wound healing process of the cornea [19]. Cisd2 regulates intracellular Ca^{2+} homeostasis and is essential to maintaining the normal structure and functioning of mitochondria in adipose, liver and heart tissue [21–25]. Both Ca^{2+} homeostasis and mitochondrial function play a crucial role in corneal biology. However, the role of CISD2 in epithelial wound healing of the cornea and the molecular mechanisms by which Ca^{2+} signaling mediates corneal epithelial proliferation and differentiation have remained elusive. Taking the above into account, the Cisd2KO mouse model is able to provide a good opportunity to use an animal model in order to gain insights into the molecular events that regulate corneal wound healing.

Our success in discovering how Cisd2 plays an essential role in the mouse cornea has also motivated us in our efforts to explore the association between human CISD2 and the clinical manifestations of ocular surface disease. Additionally, our aim has been to study the molecular mechanisms underlying the ocular phenotypes caused by Cisd2 deficiency using both the Cisd2KO mice model and a human corneal epithelial cell (HCEC) platform that has a CRISPR-mediated CISD2KO background. Furthermore, to extend our mechanistic findings into a translational application, we have developed a potential therapeutic strategy that targets Ca^{2+} signaling. Such signaling has been found to be dis-regulated in the corneal epithelium when ocular surface disease is present. The aim of this translational strategy is to identify ways of promoting epithelial regeneration and accelerating corneal wound healing.

2. Methods

2.1. Human corneal tissue samples, peripheral blood samples and clinical evaluation

Corneoscleral buttons isolated from human donor or recipient eyes were obtained from the Keelung Chang Gung Memorial Hospital Eye Bank. The written informed consent from the donor for the use in research was waived by the IRB. The corneal tissues were used to investigate the expression of CISD2 protein by immunofluorescence staining. Human peripheral white blood cells were collected from patients with corneal pathologies and normal volunteers visiting Ophthalmology outpatient clinic to detect CISD2 mRNA levels. We also conducted a retrospective study to enroll patients followed at a single institution (Keelung Chang Gung Memorial Hospital) with moderate to severe dry eye disease (DED) (cornea fluorescein staining score of 3, 4 or 5 by the modified Oxford scale) [26], who had

Significant corneal scarring reduces the light passing through the cornea to the retina and causes the cornea to appear white or cloudy, in other words there is corneal opacity present. Ultimately, this leads to functional vision loss. According to the World Health Organization, corneal opacity is the fourth leading cause of blindness worldwide. Globally, it is estimated that at least 4.2 million people (5.1%) have vision impairments due to corneal opacity [4]. The formation of corneal scars is closely related to the process of corneal wound healing, which is quite complicated, and includes active migration of superficial cells to seal the denuded surface, limbal epithelial cell proliferation and stratification, the reassembly of adhesion molecules, and the remodeling of the extracellular matrix, as well as a series of interactions between cytokines, corneal epithelial cells and stromal cells [5].

Several lines of evidence indicate that Ca^{2+} -dependent signaling and cytoskeletal rearrangement are essential for proper wound repair of the corneal epithelial layers [6,7]. The extracellular Ca^{2+} concentration and various Ca^{2+} -linked proteins have been demonstrated to affect both the proliferation and differentiation of corneal epithelial cells using mice and bovine models [8,9]. In addition, previous studies have revealed that an increased intracellular Ca^{2+} concentration inhibits epithelial proliferation and promotes epidermal-like differentiation in the mouse cornea [8,10]. Furthermore, hypercalcemia appears to retard corneal wound healing in ovariectomized rats, while, using human corneal epithelial cells, an enhanced intracellular Ca^{2+} level results in a decrease in cell viability [11]. These findings are consistent with the clinical observation that chelation of Ca^{2+} with the topical application of ethylene-diamine-tetra-acetic acid (EDTA) is an effective way of treating band keratopathy [12,13]. However, it is not

inadequate response to twice-daily use of 0.05% cyclosporine A (CsA) and then switched to once daily 0.1% CsA. Patients who were younger than 18, contact lens wearer, with a history of ocular trauma, infection, inflammation other than DED within 3 months of study period were excluded. They had a 2-month treatment with 0.1% CsA and were then shifted back to twice daily 0.05% CsA. Objective and subjective parameters including fluorescein tear breakup time (TBUT), Schirmer's test (without anesthesia), cornea fluorescein score (CFS) grading, cornea sensitivity assessment with Cochet-Bonnet aesthesiometer, and Ocular Surface Disease Index (OSDI) questionnaire were used to evaluate the treatment response. All the clinical investigations have been conducted according to the statement of Declaration of Helsinki.

2.2. Mouse models

Cisd2KO mice were generated as previously described [19]. Female mice were employed for all experiments. All mice have a congenic C57BL/6 background and were bred and housed in a specific pathogen-free facility with a 12 hr light/12hr dark cycle at persistent room temperature (20–22°C) and allowed ad libitum access to food and water.

2.3. Ethics

The human studies were approved by the Institutional Review Board (approval no. 201509558B0, 201900646B0, 20200799B0, 202001685B0) at Chang Gung Memorial Hospital, Taiwan. The animal protocols were approved by the Institutional Animal Care and Use Committee of Chang Gung Memorial Hospital (approval no. 2015121606, 2020092211) and National Yang-Ming University (approval no. 1021218).

2.4. Corneal surgery for wound healing study

The 12–14-week old Cisd2KO and WT C57BL/6 female mice were studied. With the subject under general anesthesia, the corneal epithelium was removed using an Alger Brush in anesthetized mice; a 1.5-mm diameter corneal epithelial defect was made in the right eye (OD) and left eye (OS). Care was taken not to injure the corneal stroma. The injured corneas were stained with fluorescein (Fluoro Touch) following manufacture's standard protocol and photographed with slit lamp daily for 17 or 13 days after the injury, and the size of the injured area was measured on the images with technical illustration and graphic software (Image J). For the cyclosporine A treatment, one day after mice corneal surgery, the RESTASIS® (0.05% cyclosporine A) and 0.9% normal saline (NS) was treated in OD and OS, respectively, twice a day for 17 days, then sacrificed mice and collected the corneal tissues for further analysis. For the EDTA treatment, one day after mice corneal surgery, the 0.1% EDTA (in 0.9% normal saline) and NS was treated in OD and OS, respectively, twice a day for 13 days, then sacrificed mice and collected the corneal tissues for further analysis.

2.5. Histopathology

Mouse corneas were collected, fixed with 10% formalin buffered with phosphate, underwent tissue processing and embedded in paraffin. H&E and Masson's trichrome staining (Muto Pure Chemicals) of tissue sections (3 μm) were conducted using standard protocols.

2.6. Immunofluorescence (IF) staining

In brief, at least 15 consecutive, three-micrometer-thick, 10% formalin-fixed, paraffin-embedded sections taken from human central corneas or mouse corneas were mounted on silane-coated slides.

These sections were dewaxed in xylene and then rehydrated through graded alcohol. Antigen retrieval was performed by adding proteinase K. To block nonspecific staining, each slide was incubated in saline containing 2% BSA. Sections were then rinsed in deionized water followed by Tris buffer. Immunofluorescent staining was carried out using the following primary antibodies: Cisd2 [19,22], Keratin 12 (24789-1-AP, Proteintech), CD45 (GTX116018, GeneTex), Ki-67 (AB9260, Millipore) and BrdU (51-75512L, BD Pharmingen). Each entire immunofluorescent stained section was co-stained with Hoechst 33342 (H3570, Invitrogen) nucleic acid stain. Prepared sections were subjected to confocal microscope (Leica, Germany) at a magnification of 630x. To better demonstrate the differential expression in patients with the various different corneal diseases, we analyzed the intensity of K12 and Cisd2 immunofluorescence of each human corneal section using MetaMorph microscopy automation and Image analysis software (Leica, Germany). The region of interest (ROI) was automatically labeled and the intensity of each target protein was counted and averaged against the total pixels of the ROI.

2.7. Transmission electron microscopy (TEM)

The mouse corneas were dissected and fixed in a mixture of 1.5% glutaraldehyde and 1.5% paraformaldehyde in 100 mM cacodylate buffer (pH 7.3). Corneal tissues were post-fixed in 1% OsO₄ and 1.5% potassium hexanoferrate, and then rinsed in cacodylate and 200 mM sodium maleate buffers (pH 6.0) followed by block-stained with 1% uranyl acetate. Following dehydration, the corneas were embedded in EMBED 812 resin (14120, EMS) and sectioned for TEM as described previously [27].

2.8. HCEC cell culture and generation of the HCEC Cisd2 KO cell line

The human corneal epithelial cells (HCEC) cell line (ATCC, CRL-11515) was cultured in HCEC complete medium (keratinocyte serum free medium [17005-042, GIBCO] with 5 ng/ml human recombinant EGF, 0.05 mg/ml bovine pituitary extract, 0.005 mg/ml insulin and 500 ng/ml hydrocortisone) and maintained in a humidified incubator at 37°C with 5% CO₂. The Cisd2 gene was disrupted in HCEC cells by CRISPR/Cas9n (D10A) method [28]. The following is the single guide RNA (sgRNA) sequence lists sgRNA1: CAGCACCATCTGGCCAG, sgRNA2: CGTGGCCCGTATCGTGA. The sgRNA/Cas9n (D10A) expression vector was obtained from Cancer Progression Research Center-Genome Editing Core Facility, NYCU. The sgRNA1/Cas9n and sgRNA2/Cas9n plasmids express RFP and EGFP, respectively. The sgRNA1/Cas9n and sgRNA2/Cas9n plasmids were co-transfected into HCEC cells by PolyJet™ reagent (SignaGen Laboratories). The EGFP/RFP double positive cells were sorted by BD FACSAria™ IIu flow cytometry. Sorted cells (5,000 or 10,000 cells) were seeded in 10-cm dishes and incubated with 5% CO₂ at 37°C until the colony formed. The colonies were picked and amplified in 24-well plate. The Cisd2 KO cells were examined by PCR and DNA sequencing, as well as western blot analysis.

2.9. Lentivirus-mediated Cisd2 re-expression (Cisd2RE)

The mouse Cisd2 expression vector was packaged into the lentivirus. The lentivirus preparation and production was conducted by the National RNAi Core Facility at Academia Sinica in Taiwan. The Cisd2KO HCEC cells were seeded before the day of lentiviral infection. After the overnight cultured, the lentivirus with polybrene (8 μg/ml) was added into the culture medium. After 24 hr infection, the medium contain lentivirus was removed and wash twice by PBS. The post-infected cells were selected by puromycin (3 μg/ml). The incubation and recovery times were depended on the selection efficiency and the following experiments.

2.10. Western blotting

HCEC cells were homogenized in RIPA buffer (50 mM Tris at pH 7.4, 150 mM NaCl, 1% Triton X-100, 0.5% Sodium deoxycholate, 0.1% SDS with complete protease inhibitor and phosphatase inhibitor cocktails [Roche]) and denatured in SDS sample buffer (50 mM Tris at pH 6.8, 1.5% beta-mercaptoethanol, 2% SDS and 10% glycerol) for 10 min at 100°C. The total protein extracts were separated by SDS-polyacrylamide gel electrophoresis (Bio-Rad) and electro-transferred to a polyvinylidene fluoride (PVDF) membrane (PerkinElmer). The membranes were blocked with 5% (w/v) nonfat dry milk, probed with Cisd2 antibody [19,22], and detected by an ECL (34580, Thermo).

2.11. Intracellular calcium imaging

Cytosolic Ca^{2+} was measured at 37°C using the fura-2 fluorescence ratio method on a single-cell fluorimeter. HCEC cells were loaded with 2 μ M fura-2/AM (Invitrogen, San Diego, CA) in KSF culture medium at 37°C for 30 min. ER Ca^{2+} was depleted by the addition of thapsigargin (TG) (2 μ M) for 10 min in Ca^{2+} -free buffer. Thereafter, Ca^{2+} influx by SOCE was triggered by an exchange with extracellular Ca^{2+} buffers (0 to 2 mM) for 5 min at time point "1 min". Fura-2/AM were excited alternatively between 340 nm and 380 nm using the Polychrome IV monochromator (Till Photonics, Grafelfing, Germany), and images were captured using an Olympus IX71 inverted microscope equipped with a xenon illumination system and an IMAGO CCD camera (Till Photonics). The fluorescence intensity was monitored at 510 nm, stored digitally, and analyzed using the program TILLvisION 4.0 (Till Photonics, Grafelfing, Germany).

2.12. Intracellular reactive oxygen species levels

Intracellular reactive oxygen species (ROS) levels in HCEC cells were determined using MitoSOX (M36008, Invitrogen), which is a mitochondrial targeting ROS sensitive fluorescence dye.

2.13. Measurement of mitochondrial oxygen consumption rate using a Seahorse analyzer

An XFe24 analyzer (Seahorse Bioscience, MA) was applied to measure the oxygen consumption rate (OCR) of mitochondria. The HCEC cells were cultured in a fibronectin-coated (0.01 mg/mL fibronectin, 0.03 mg/mL bovine collagen type I and 0.01 mg/mL bovine serum albumin) XF24 V7 plate at 3×10^4 cells/well. The HCEC cells were kept overnight in HCEC complete medium and then replaced by fresh HCEC complete medium (pH=7.4) at 1 hr before measurement. The OCR was measured before and after added the indicated chemicals (1 μ M oligomycin A, 2 μ M FCCP and 1 μ M rotenone with 1 μ M antimycin A) at 37°C. The results are presented in pmol/min/ μ g protein.

2.14. RNA isolation, reverse transcription and real-time quantitative PCR (qPCR) assay

Total RNA was isolated from mouse corneal tissues and human white blood cells using TRI Reagent (T9424, Sigma). The cDNA was synthesized by reverse transcription of total RNA using random hexamers with SuperScriptTM III reverse transcriptase (18080, Invitrogen) according to the manufacturer's instructions. The quantitative PCR (qPCR) using TaqMan Real-time PCR Assays (Applied Biosystems, Foster City, CA, USA) following manufacturer's standard protocol. The results were calculated with 2-CT and normalized to HPRT1.

2.15. RNA sequencing and pathway analysis

The RNA sequencing (RNA-seq) was conducted by National Yang-Ming University VYM Genome Research Center. The differentially expressed genes (DEGs) calculated from the RPKM (reads per kilobase of exon model per million reads) in RNA-Seq data. The Gene Ontology (GO) functional characterization was performed by online tools PANTHER (www.pantherdb.org) [29] and STRING (https://string-db.org) [30]. Heatmaps were graphed by loading log-transformed fold changes into MultiExperiment Viewer (MEV) 4.9 software [31].

2.16. Statistical analysis

The data are presented as mean \pm SD as described in the figure legends. Comparisons between the two groups were done using an unpaired two-tailed Student's t test. When comparisons were done among three groups or more, one-way ANOVA with Bonferroni multiple comparison test was used. Quantification of the healing rate and the light transmission in mice corneal wounding experiments was performed using generalized equation estimation (GEE). When analyzing statistical differences among groups, $p < 0.05$ was considered significant and the significances are presented as follows: * $p < 0.05$; ** $p < 0.01$; and *** $p < 0.001$. All statistical analysis was carried out using the software GraphPad Prism 8.0.

3. Role of the funding source

The funders had no role in study design, data collection, data analysis and interpretation, writing and submission of the manuscript.

4. Results

4.1. Differential expression patterns of C1SD2 in human corneal epithelial and endothelial diseases

The ocular phenotype of Cisd2KO mice, namely corneal opacity, hyperkeratinization of the corneal epithelium, neovascularization and inflammation, resembles the clinical manifestations of LSCD in human patients. To investigate the association between C1SD2 and corneal diseases, we performed immunohistochemistry (IHC) staining of human specimens obtained after routine corneal transplantation procedures. These corneal specimens were able to be separated into two groups. The first are ocular diseases that primarily involve the corneal epithelium, including corneal opacity, corneal degeneration, corneal ulceration, and abnormal stratification of corneal epithelial layers. Notably, the characteristics of LSCD, such as corneal neovascularization (red arrows), corneal opacity (yellow arrows) and corneal epithelial defects, can be observed in these patients. The second are ocular diseases that primarily involve the corneal endothelial layers, such as pseudophakic bullous keratopathy and endothelial graft rejection. The second group of patients has relatively normal epithelial stratification of their cornea (Fig. 1a, b). Intriguingly, C1SD2 is undetectable by IF staining through the entire epithelial layer of corneas of patients with an epithelial problem; on the other hand Keratin 12 (K12), a marker for corneal epithelium, is able to be detected in all of the corneal specimens at various levels of expression. Conversely, both C1SD2 and K12 are expressed at a significant level in the epithelial layers of ocular diseases that primarily affect the corneal endothelium (Fig. 1c, d and Supplementary Fig. 1a-d).

To delineate whether the differential expression pattern of C1SD2 occurs in a tissue-specific manner, namely it is specific to the corneal epithelium or, alternatively, there is a systemic effect throughout the body, we analyzed the C1SD2 mRNA level of white blood cells (WBCs) using blood samples collected from patients with either corneal epithelial disease or corneal endothelial disease, as well as normal

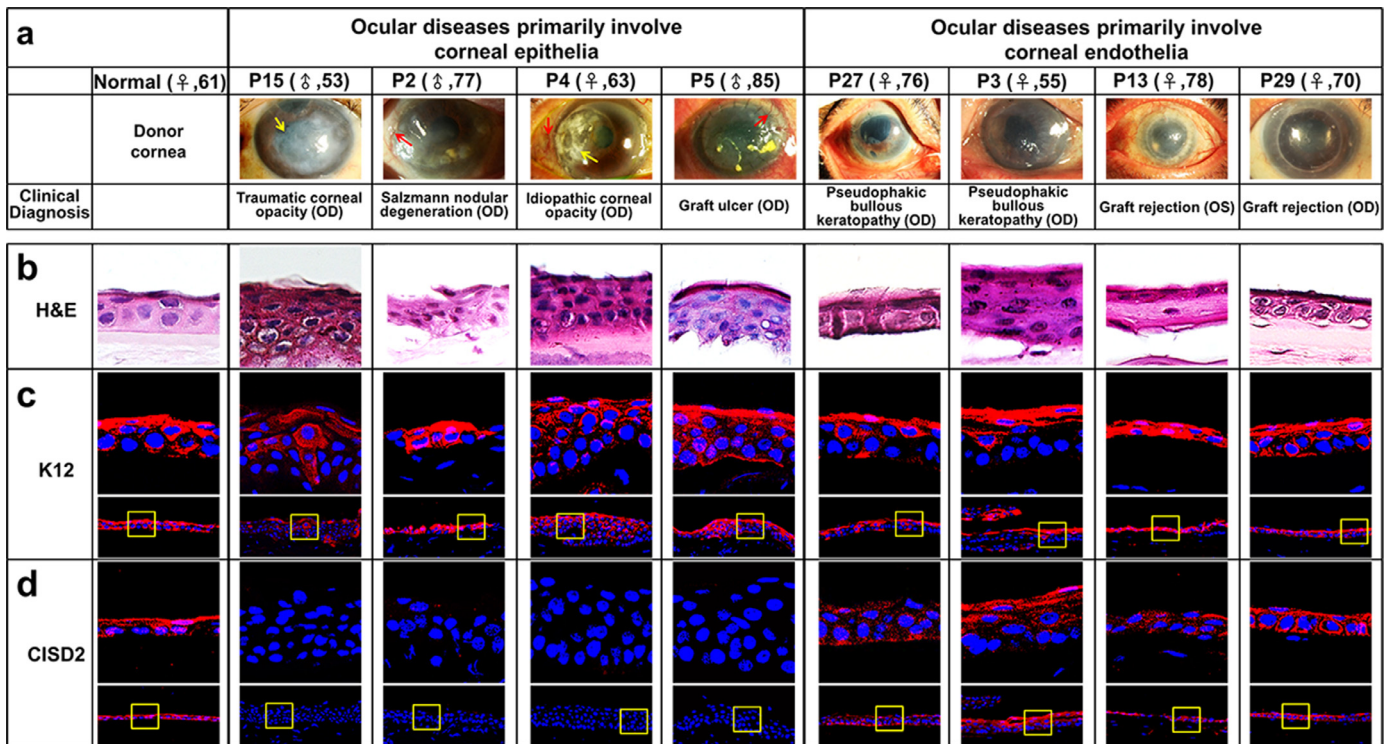


Fig. 1. The differential expression patterns of CISD2 in human ocular diseases primarily involve corneal epithelium or endothelium. (a) External eye photographs collected from corneoscleral buttons in patients underwent corneal transplantations. A 61 years old female donor was served as the normal control. Clinical diagnoses that primarily involve corneal epithelium included traumatic and idiopathic corneal opacities, Salzmann nodular degeneration and graft ulcer with the presentations of opacities (yellow arrows) and corneal neovascularization (red arrows). Pseudophakic bullous keratopathy and graft rejection accounted for lesions predominantly affected corneal endothelium resulting in corneal edema and bullae formation. Yellow arrows indicate opacity; red arrows indicate corneal neovascularization. (b) H&E stain. Abnormal corneal epithelial stratification was observed in patients primarily involve pathological conditions in the corneal epithelium. (c) IF staining of K12, a marker for corneal epithelial cells. K12 is universally present in the epithelial layer of patients with corneal endothelial lesions; however, it is variably expressed in patients with corneal epithelial diseases. (d) IF staining of CISD2. CISD2 expression is nearly abolished in ocular diseases primarily involve corneal epithelium; however, CISD2 is detected in ocular diseases primarily involve corneal endothelium. In (c) and (d), the upper panels are magnification of the insets (yellow square) shown in the lower panels. P indicates patient.

subjects who had visited our Ophthalmology Outpatient Clinic, but were without any ocular disease. Quantification by real-time RT-qPCR revealed that there was no significant difference in the CISD2 mRNA levels of the WBCs of ocular patients with either epithelial or endothelial problems affecting their cornea (Supplementary Fig. 1e). This indicates that the dramatic reduction in CISD2 expression in the former patients appears to involve tissue-specific regulation rather than a systemic effect that affects the whole organism.

4.2. *Cisd2* deficiency induces ocular surface abnormalities and retards corneal epithelial wound healing

To further verify if the corneal abnormalities induced by *Cisd2* deficiency are similar to the clinical manifestations of human LSCD, we carry out detailed ocular phenotyping of *Cisd2*KO mice. In WT mice, their corneas are clear and show negative staining with fluorescein; on the other hand, in *Cisd2*KO mice, their corneas display a LSCD-like phenotype, namely corneal opacity, neovascularization, surface keratinization, and epithelial damage, as indicated by the penetration of fluorescein dye (Fig. 2a). It is worth noting that female *Cisd2*KO mice show an earlier onset of these ocular surface abnormalities, which implies a possible role for hormonal effects in this model. Therefore, from this point onwards, we used the females for the study in order to obtain a stable ocular surface phenotype. In WT mice, their corneal epithelia are composed of three to five layers, including the surface epithelium, the wing cell layer and basal epithelium; the normal stratification of the corneal epithelia and rectangularly arranged stromal collagen fibers can be seen using H&E and Masson's trichrome staining (Fig. 2b). However, in *Cisd2*KO mice, an

irregular corneal surface and abnormal epithelial stratification were observed. Additionally, opacity, which is likely due to the deposition of keratin-like debris outside the cornea, can also be detected. This type of lesion is usually associated with accelerated epithelial differentiation and is likely to impair vision. Furthermore, *Cisd2* deficiency also results in corneal thickening, a disorganized arrangement of collagen fibers and the presence of cellular infiltration within the corneal stroma (Fig. 2b). Moreover, IHC staining of CD45 reveals a strong positive signal for leukocyte-derived inflammatory cells within the central cornea and limbal areas, which indicates severe inflammation of the cornea of the *Cisd2*KO mice (Fig. 2c). In addition, corneal epithelial layers are normally maintained in dynamic equilibrium by the continuous shedding of epithelial cells from the surface and the replacement of these cell by renewal via stem cells from the limbus; these stem cells are located at the junction between cornea and conjunctiva. Terminal differentiation of cells, coupled with cell death by apoptosis, prompts this cell loss via desquamation, a process aided by eyelid blinking [32]. Interestingly, the presence of accelerated desquamation and increased shedding of the outer layer of the cornea raises the possibility that the efficient replenishment of the corneal epithelium by limbal stem cells is compromised in *Cisd2*KO mice. Normally, K12 is detected across the entire corneal epithelium and the suprabasal limbal epithelium; however, K12 was not expressed in either the limbal basal epithelium or the adjacent conjunctiva [33]. Notably, IF staining of K12 was found to be less intense in the *Cisd2*KO cornea compared to the WT cornea (Fig. 2d). This indicates that an abnormal differentiation process is likely to be occurring in the corneal epithelium of *Cisd2*KO mice.

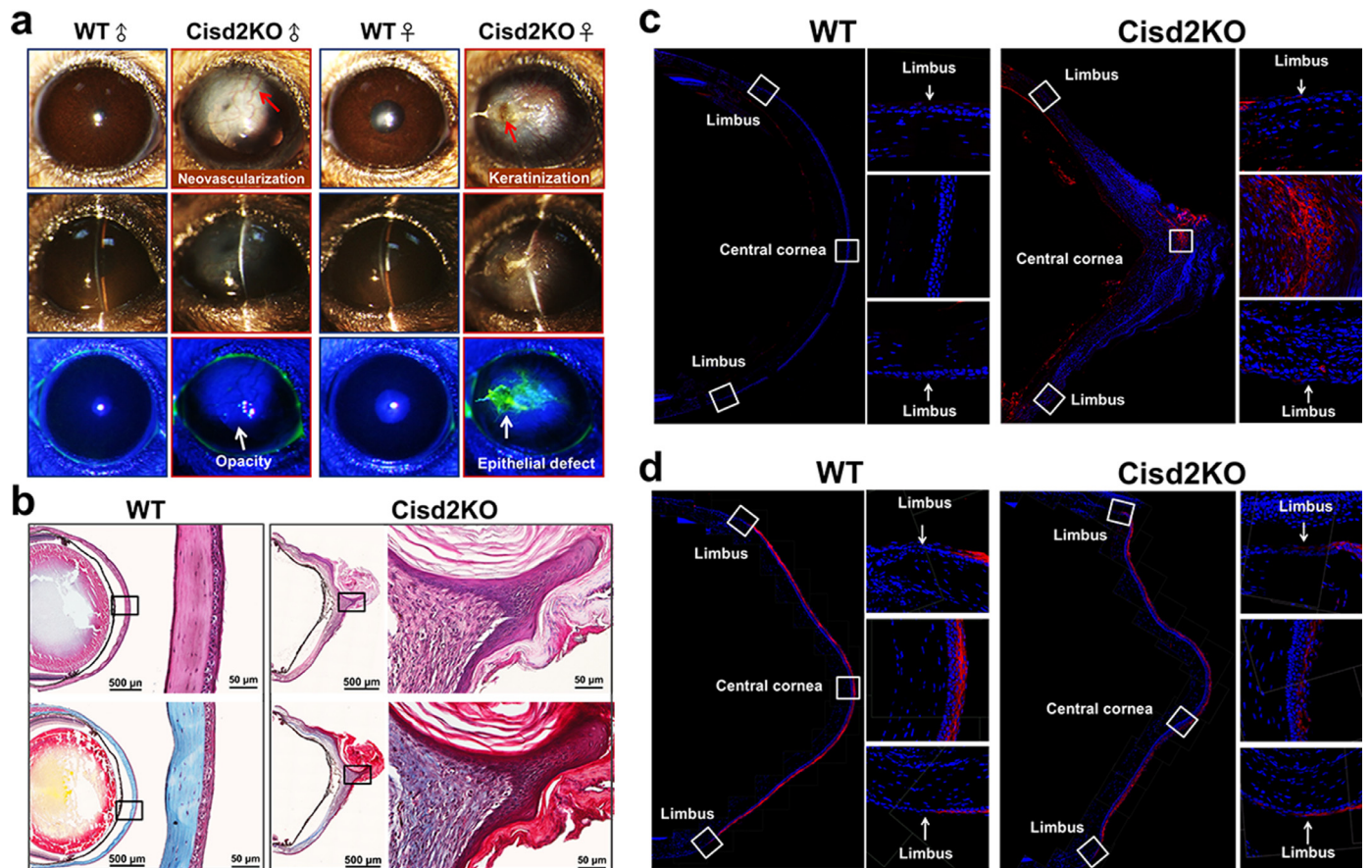


Fig. 2. *Cisd2* deficiency causes ocular surface abnormalities and retards corneal epithelial wound healing. (a) In WT mice, their corneas are clear and fluorescein reveals negative staining. In contrast, in *Cisd2*KO mice at 4–6 months old, various ocular surface abnormalities including corneal neovascularization, surface keratinization, corneal scarring and epithelial defect (arrows) are noted. (b) In WT mice, normal stratification of corneal epithelia and rectangular alignment of corneal stromal collagen layers are well demonstrated by H&E and Masson's trichrome staining. In *Cisd2*KO mice, however, exaggerated epithelial thickening, abnormal epithelial stratification, loss of stromal collagen rectangular alignment with cellular infiltration, increased neovascularization and surface keratinization are found in their corneas. These corneal sections are prepared from 4-month old mice. (c) IF of CD45, a leukocyte common antigen, is barely seen in WT cornea. In *Cisd2*KO mice, however, strong signal of CD45 is detected in the central corneal epithelia and weakly present in the limbal areas. (d) IF staining of K12, a marker for corneal epithelial wing cells, shows a relatively stronger signal in the WT cornea compared to *Cisd2*KO cornea.

4.3. *Cisd2* deficiency impairs epithelial wound healing of the cornea and this leads to exhaustion of progenitor cells in the limbus

To carry out a longitudinal study and to observe changes to the ocular surface, we use fluorescein to detect corneal damage. A positive green staining indicates the presence of damage to the cornea and this occurs when the dye is able to penetrate the surface. In WT mice, their cornea remains clear and is negative for fluorescein staining. On the other hand, in the *Cisd2*KO mice, surface roughness and multiple area of erosion could be noted affecting the corneal epithelium at 6-mo, and this phenotype became exacerbated at 9-mo (Fig. 3a). Normally, in response to external insults to the cornea, limbal stem cells proliferate and then migrate centripetally in order to heal the injured area and they then gradually become terminally differentiated cells. The whole process is traditionally recognized as the “X-Y-Z” hypothesis [1], wherein X represents the proliferation and stratification of the limbal basal cells, Y stands for the centripetal migration of the basal cells and Z delineates the desquamation of the superficial cells. Intriguingly, IF staining of Ki67, which is a nuclear protein associated with cellular proliferation, reveals that, in *Cisd2*KO mice, Ki67-positive cells are able to be detected in multiple layers and these cells are distributed throughout the entire central epithelial region of the cornea; this contrasts sharply with the pattern in WT cornea, where Ki67-positive cells are located in the limbus and basal epithelial layer (Fig. 3b). These findings suggest that *Cisd2*

deficiency brings about an abnormal enhancement of epithelial proliferation across the cornea of *Cisd2*KO mice.

It is generally believed that stem cells eventually lose their ability to proliferate in older animals. However, little is known about whether the epithelial progenitor cells located in the limbus undergo such a phenomenon; specifically, we would like to know whether exhaustion of these epithelial progenitor cells is accelerated in pre-maturely aged *Cisd2*KO mice. To test this possibility, we use bromodeoxyuridine (BrdU) to label the epithelial progenitor cells; BrdU is an analog of thymidine that is able to be incorporated into the newly synthesized DNA present in replicating cells. Interestingly, in *Cisd2*KO mice, there is a significant increase in corneal BrdU-positive cells at 3-mo and 6-mo; however, by way of contrast, the presence of BrdU-positive cells is significantly decreased and barely detectable at 9-mo, all cases compared with WT corneas (Fig. 3c and Supplementary Fig. 2). These findings indicate that at a younger age (namely 3-mo and 6-mo), the limbal progenitor cells are continuously activated and proliferating in response to the corneal microtrauma that appears consistently to occur in *Cisd2*KO cornea; at a later stage (e.g. 9-mo), the limbal progenitor cells eventually have become exhausted and are unable to replenish the cornea with new epithelial cells. As a consequence it seems that a vicious cycle is present in the *Cisd2*KO cornea, whereby persistent corneal damages bring about continued stimulation of repair and this cycle eventually results in depletion of the limbal progenitor reservoir and pathological keratinization (Fig. 3d).

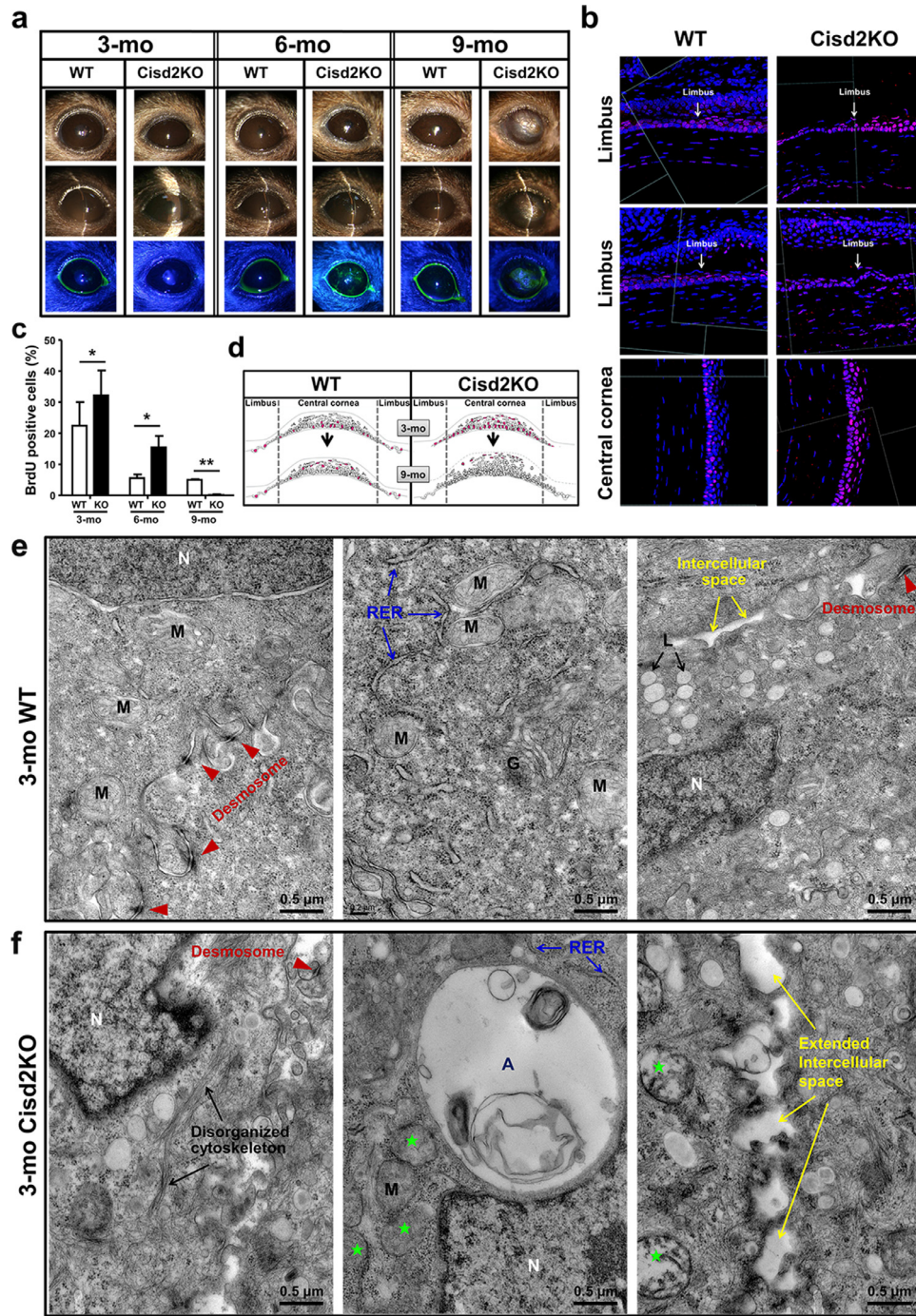


Fig. 3. Cisd2 deficiency in the cornea causes poor epithelial wound healing and results in limbal progenitor cell exhaustion. (a) In WT mice at all ages, their corneas remained clear and fluorescein showed a negative staining. However, in Cisd2KO mice, corneal epithelial erosion is noted at 6-mo mice and persistent corneal epithelial defects, corneal opacity and neovascularization are found at 9-mo mice. (b) Ki67, a cell proliferation marker, is normally expressed in the basal layer of corneal and limbal epithelial cells of 3-mo WT mice. However, in 3-mo Cisd2KO mice, Ki67 is detected in almost every layer through the whole limbal and corneal epithelia. This indicates that an active cell proliferation is induced in response to the persistent corneal epithelial wounds. (c) Quantification of BrdU-positive cells within corneal epithelia by IF staining (n=3). Cisd2KO mice and their WT littermates at 3-, 6- and 9-mo are subjected to daily intraperitoneal injections of 50 mg/kg BrdU for 9 consecutive days. The mice are sacrificed and their corneas were cross-sectioned 24 h after receiving the last BrdU injection. Data are presented as the mean \pm SD. * $p < 0.05$; ** $p < 0.01$ by Student's t-test. (d) This cartoon summarizes the observation that leads to the hypothesis of limbal progenitor cell exhaustion in Cisd2KO mice. In the cornea of WT mice, the epithelial progenitor cells reside in the limbal areas and replenish the shedding corneal epithelial cells by the traditional X-Y-Z centripetal migration. In the cornea of Cisd2KO mice, limbal progenitor cells are continuously activated and differentiated into post-mitotic and terminally differentiated cells in response to a chronic damage and an impaired wounding repair process. As a result, the limbal progenitor cells are gradually depleted and ultimately exhausted, leading to LSCD. (e) TEM analyses reveal a variety of ultrastructural abnormalities in the cornea of Cisd2KO mice. In WT cornea (upper panels), high density of desmosomes (red arrow heads) and abundant rough ERs (blue arrows) are evenly distributed; in addition, the intercellular space is relatively narrow (yellow arrow). Notably, in Cisd2KO cornea (lower panels), the number of desmosomes (red arrow heads) is apparently decreased, leading to the formation of an extended intercellular space (yellow arrows) between epithelial cells. In addition, decreased number of rough ERs (blue arrows), degenerating mitochondria with disintegrating cristae (green stars) as well as the disorganized cytoskeleton (black arrows) are detected. A, autolysosome with membrane debris; G, Golgi apparatus; L, lipid droplet-like structure; M, mitochondria; N, nucleus; RER, rough ER; ★ indicates disintegrating cristae. Magnification: 30,000X.

To characterize the ultrastructural changes that occur in corneal epithelial cells, we carried out an examination using transmission electron microscopy (TEM). Notably, in the WT cornea, there is a high density of desmosomes; these serve as intercellular junctions and provide strong adhesion between epithelial cells. Furthermore, intact mitochondria, rough endoplasmic reticulum (RER) and Golgi apparatus are easily detectable (Fig. 3e). On the other hand, in the Cisd2KO cornea, there is a significant decrease in the number of desmosomes present in the epithelial cells and this seems to create a much larger intercellular space between epithelial cells. In addition, within the epithelial cells of Cisd2KO cornea, a variety of ultrastructural abnormalities are able to be detected, including a disorganized cytoskeleton, degenerating mitochondria with disintegrating inner cristae, and a decrease in RER density, as well as the formation of large autolysosomes that contain membrane debris (Fig. 3f).

4.4. Cisd2 deficiency disturbs intracellular Ca²⁺ homeostasis, impairs mitochondrial function and increases the oxidative stress level of HCEC cells

Our previous studies have demonstrated that Cisd2 regulates intracellular Ca²⁺ homeostasis [21–23]. Based on these findings, we attempted to assess the effect of Cisd2 deficiency on intracellular Ca²⁺ homeostasis in a human corneal epithelial cell (HCEC) line. Two HCEC lines were created, a Cisd2KO line, and a Cisd2RE line, the latter being a Cisd2KO line with re-expression (RE) of Cisd2; these modified cell lines were examined by Western blotting (Fig. 4a). It was noted that the basal cytosolic Ca²⁺ level in the HCEC-Cisd2KO cells was significantly elevated compared to HCEC-WT cells; this contrasted with the situation in the Cisd2RE cells where the abnormal elevation of cytosolic Ca²⁺ was reversed and the level was similar to that found in the HCEC-WT cells (Fig. 4b, c). Additionally, we examine the responses of HCEC to capsaicin (an active component of chili peppers) and histamine (a compound involved in the local immune response), both of which are usually used to study changes in intracellular free Ca²⁺ concentrations, namely in terms of Ca²⁺ efflux from the ER lumen, and in terms of extracellular Ca²⁺ influx, respectively (Fig. 4d–g). Remarkably, a significant downregulation of both the capsaicin-evoked and histamine-evoked cytosolic Ca²⁺ elevations was found in the HCEC-Cisd2KO cells compared to both the HCEC-WT and the HCEC-Cisd2RE cells. These findings indicate that Cisd2 deficiency brings about a disruption of normal Ca²⁺ related cellular responses via a dysregulation of Ca²⁺ signaling (Fig. 4e, g).

Store-operated Ca²⁺ entry (SOCE) is a major mode of Ca²⁺ influx in non-excitable cells and is involved in regulating multiple cellular functions, including cell proliferation, focal adhesion turnover, and cell migration. Stromal-interaction molecule 1 (STIM1) is the major Ca²⁺ sensor in the ER; STIM1 aggregates into multiple puncta in order to trigger the SOCE, during which Ca²⁺ is depleted in the ER. Normally, thapsigargin-mediated SERCA inhibition blocks the uptake of Ca²⁺ from the cytosol into ER via SERCA, but allows Ca²⁺ to flow from the ER into the cytosol. As a consequence, this is able to trigger a sustained elevation of cytosolic Ca²⁺ level via the SOCE in HCEC-WT cells (Fig. 4h). However, in the HCEC-Cisd2KO cells, there is a significantly lower Ca²⁺ influx after thapsigargin treatment (Fig. 4i), which suggests that there may be defects affecting the SOCE machinery. Furthermore, confocal imaging was able to reveal that most of the activated STIM1 proteins aggregate into puncta when under Ca²⁺ depletion induced by thapsigargin, in both the HCEC-WT and HCEC-Cisd2RE cells, but this does not occur in the HCEC-Cisd2KO cells under similar conditions (Fig. 4j). These findings reveal that Cisd2 deficiency leads to an impaired SOCE response in the HCEC.

Moreover, previously, we have demonstrated that an increase in cytosolic Ca²⁺ level induces Ca²⁺-calcineurin-dependent signaling and this inhibits adipogenesis in Cisd2KO cells and, furthermore,

that inhibition of calcineurin by cyclosporine A (CsA) restores this phenotypic defect [21]. Intriguingly, in the HCEC-Cisd2KO cells, CsA treatment also corrects both abnormalities, namely the elevation of the basal cytosolic Ca²⁺ level and the impairment of the SOCE response (Fig. 4k, l). Since CsA has an effect on both the calcineurin and the mitochondrial permeability transition pore (mPTP), we next used FK506, which is a specific inhibitor of calcineurin that does not affect the mPTP, to validate if it is the calcineurin-dependent signaling pathway specifically that is involved in the abnormalities caused by the disrupted Ca²⁺ homeostasis. Remarkably, we found that FK506 indeed has a profound effect, similar to CsA, namely that it reduces the basal cytosolic Ca²⁺ level and increases SOCE activity in the HCEC-Cisd2KO cells (Supplementary Fig. 3a, b). Moreover, we also found that there is no significant difference in the mPTP status in the HCEC cells with a WT, Cisd2KO or Cisd2RE background (Supplementary Fig. 3c). Together, these results indicate that an increase in cytosolic Ca²⁺ level induces Ca²⁺-calcineurin-dependent signaling and that inhibition of calcineurin by CsA or FK506 appears to restore the phenotypic defect in the HCEC-Cisd2KO cells.

Elevation of cytosolic Ca²⁺ usually activates the mitochondrial uniporter system, which lead to mitochondrial Ca²⁺ overload and results in a variety of detrimental effects [21–23]; these include mitochondrial dysfunction and increased oxidative stress. Interestingly, we found that mitochondrial function is compromised in the HCEC-Cisd2KO cells, as shown by a reduction in their oxygen consumption rate (OCR) (Fig. 4m, n). Furthermore, we used mitoSOX, a fluorescent probe of mitochondrial reactive oxygen species (ROS), to evaluate the levels of oxidative stress. Our results revealed that there was a significant increase in mitochondrial ROS in HCEC-Cisd2KO cells (Fig. 4o). Importantly, in HCEC-Cisd2RE cells, their OCR and mitoSOX intensity are both restored to a level similar to that of the HCEC-WT cells (Fig. 4m–o), indicating that these detrimental effects are indeed caused by Cisd2 deficiency. To delineate the role of Cisd2 in corneal regeneration, which is known to involve a number of complex cellular events, we carry a series of analyses including cell proliferation, cell migration by wound healing and Transwell assays, as well as an analysis of focal adhesion distribution. In the HCEC-Cisd2KO cells, their proliferation was found to be significantly decreased (Fig. 4p); in addition, their migration ability was also significantly reduced, as revealed by both 2D wound healing assays (Fig. 4q) and the 3D Transwell migration assays (Fig. 4s). Remarkably, in the HCEC-Cisd2KO cells, both CsA and FK506 are able to improve cell migration ability as measured by 2D and 3D migration assays (Fig. 4r–t and Supplementary Fig. 3d–f); this is in agreement with the observation whereby CsA and FK506 in the HCEC-Cisd2KO cells are able to downregulate cytosolic Ca²⁺ levels and upregulate the SOCE (Fig. 4k, l and Supplementary Fig. 3a, b). Additionally, the intracellular Ca²⁺ chelator BAPTA-AM also has a potential to reduce the cytosolic Ca²⁺ level thereby promoting the cell migration ability of the HCEC-Cisd2KO cells. However, EDTA and EGTA, two extracellular Ca²⁺ chelators, have no effect on the cell migration phenotypic defect present in the HCEC-Cisd2KO cells (Supplementary Fig. 3f).

The activation of calcineurin was further confirmed by examining the calcineurin-mediated dephosphorylation of the transcription factor NFAT1. In the HCEC-Cisd2KO cells, the elevated cytosolic Ca²⁺ level appears to activate the phosphatase activity of calcineurin and this dephosphorylates the NFAT1 transcription factor, which leads to the translocation of NFAT1 into the nucleus and this turns on expression of its downstream target genes (Supplementary Fig. 3g). Quantification of the nuclear translocation of NFAT1 shows that the nuclear/cytoplasm ratio of NFAT1 is significantly higher in HCEC-Cisd2KO cells compared with HCEC-Cisd2WT and HCEC-Cisd2RE cells (Supplementary Fig. 3h). In addition, the mRNA levels of the target genes of NFAT1, namely Nr4a1, Tnf and Cdk4, are up-regulated in the wounded corneal tissues of the Cisd2KO mice (Supplementary Fig. 3i). These results reveal that Cisd2 deficiency increases cytosolic Ca²⁺

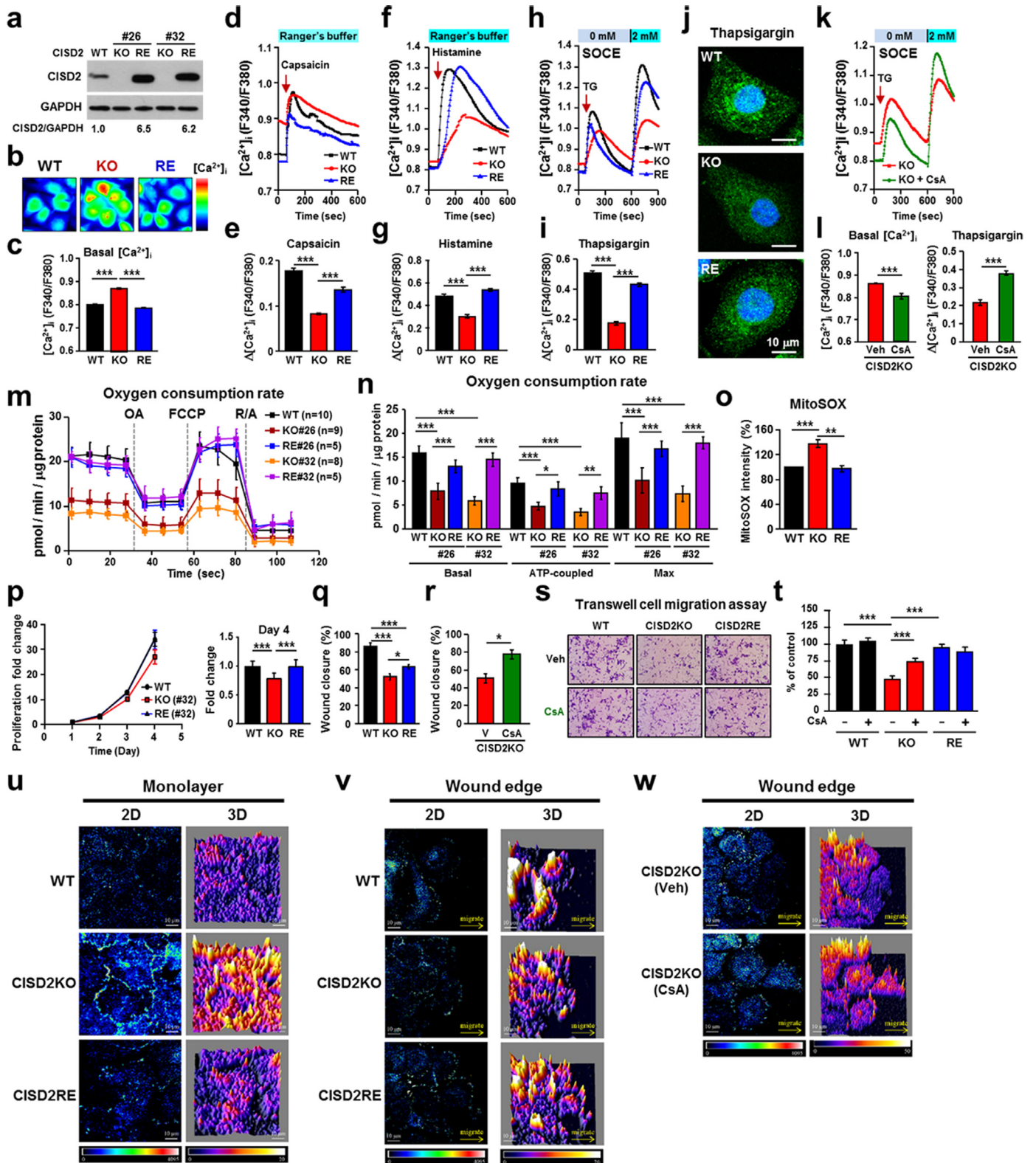


Fig. 4. Cisd2 deficiency disturbs intracellular Ca^{2+} homeostasis and impairs mitochondrial function in HCEC cells. (a) Western blot analysis of Cisd2 in HCEC carrying different genotypes, namely WT, Cisd2KO, and Cisd2RE. GAPDH is used as the internal control. Clone #26 and clone #32 are different subclones of HCEC with Cisd2KO background. (b) Representative pseudocolored fluorescence images are taken under a single cell fluorimeter. (c) Quantification of relative concentrations of basal cytosolic Ca^{2+} ($[Ca^{2+}]_i$) in HCEC cells (WT, Cisd2KO and Cisd2RE). (d) Capsaicin-evoked cytosolic Ca^{2+} elevation. Representative curves (d) and quantification of $[Ca^{2+}]_i$ (e) are recorded in Ranger's buffer following 5 μ M capsaicin stimulation. (f) Histamine-evoked cytosolic Ca^{2+} elevation. Representative curves (f) and quantification of $[Ca^{2+}]_i$ (g) are recorded in Ranger's buffer following 100 μ M histamine stimulation. (h) Thapsigargin-triggered SOCE. Representative curves (h) and quantification of $[Ca^{2+}]_i$ (i) are recorded in two phases, namely Ca^{2+} -free buffer followed by 2 mM- Ca^{2+} buffer, after 2 μ M thapsigargin stimulation. (j) STIM1 aggregates into multiple puncta as an indicator for activation of SOCE. HCEC cells (WT, Cisd2KO and Cisd2RE) are treated by 2 μ M thapsigargin for 10 min in Ca^{2+} -free buffer. Representative images of IF-stained STIM1 are taken using a confocal microscope. Scale bars, 10 μ m. (k) Cyclosporin A restores the basal cytosolic Ca^{2+} level ($[Ca^{2+}]_i$) and improves the impaired SOCE in HCEC-Cisd2KO cells. Cells are pretreated with vehicle (Veh) or cyclosporin A (CsA, 100 nM) for 30 min before Ca^{2+} measurement. (m) Oxygen consumption rate (OCR) in HCEC cells (WT, Cisd2KO and Cisd2RE) is measured by sequentially treated with Oligomycin A (1

levels and enhances the Ca^{2+} -Calcineurin-NFAT signaling pathway in the corneal epithelial cells.

Moreover, it is well known that the distribution and dynamics of focal adhesions affects the ability of cells to migrate. When HCEC-WT and HCEC-CISD2RE cells are grown in monolayer culture, their focal adhesions are scattered throughout the cell; however, when HCEC-CISD2KO cells were examined, their focal adhesions are gathered together at the cellular junctions (Fig. 4u). When wound healing assays were carried out on HCEC-WT and HCEC-CISD2RE cells, their focal adhesions are concentrated at the front end of the wounding edge aimed toward the direction of migration; in contrast, in HCEC-CISD2KO cells, fewer focal adhesions were found at the front edge of migrating cells (Fig. 4v). Finally, consistent with the observations regarding cytosolic Ca^{2+} , SOCE and cell migration, we found that CsA is able to improve the distribution of focal adhesions, moving them towards the leading edge during cell migration (Fig. 4w).

4.5. Cyclosporine A and EDTA facilitate corneal epithelial wound healing in *Cisd2*KO mice

Accumulating evidence has supported the hypothesis that activated Ca^{2+} -associated signaling is essential to the healing of epithelial wounds in the normal cornea [6,7]. Since *CISD2* deficiency leads to Ca^{2+} dysregulation and an activation of calcineurin in HCEC, it is likely that the Ca^{2+} -calcineurin-dependent signaling is indeed involved in the impaired process of wound healing found in the *Cisd2*KO cornea. To test this possibility, we perform wound healing experiments by creating mechanical abrasion wounds of the cornea and treat the wounded corneas with CsA to inhibit the calcineurin signaling pathway and we then studied the associated phenotypic effects. In WT mice, the corneal wounds were found to be almost completely repaired by day 7 after wounding when the mice were treated with CsA or with normal saline (NS) as the control (Fig. 5a). However, in *Cisd2*KO mice (the NS control group), a persistent epithelial defect with mild corneal hazing could be seen until day 17 after wounding. Intriguingly, CsA treatment was able to significantly facilitate epithelial wound healing of the cornea of *Cisd2*KO mice (Fig. 5b). Furthermore, light transmission through the corneas was also significantly improved in the CsA-treated *Cisd2*KO mice compared to the NS-treated *Cisd2*KO mice, indicating a functional improvement in corneal clarity (Fig. 5c). Remarkably, a pathological examination of the corneas revealed that CsA treatment appears to bring about recovery of the cornea to a relatively normal histology without epithelial keratinization. Moreover, CsA treatment was found to ameliorate inflammation, as evidenced by a decrease in the numbers of CD45-positive cells (Fig. 5d). Very similar findings were found when this wound healing experiment was carried out on *Cisd2*KO corneas treated with EDTA (Supplementary Fig. 4). EDTA is a Ca^{2+} chelating agent and previous studies have shown that it is often able to improve visual acuity and ocular comfort when band keratopathy is present [12,13]. In the corneal epithelium of *Cisd2*KO mice, the action of EDTA to downregulate the cytosolic Ca^{2+} level may involve the following mechanism. Cytosolic Ca^{2+} is actively transported out of the cells by two carrier

proteins, namely the plasma membrane Ca^{2+} -ATPase (PMAC) and the $\text{Na}^+/\text{Ca}^{2+}$ exchanger (NCX), to maintain a low cytosolic Ca^{2+} concentration (50–100 nM). EDTA is able to chelate extracellular Ca^{2+} , which leads to a reduced extracellular Ca^{2+} level thereby inhibiting Ca^{2+} influx into the cells. In addition, EDTA can also chelate Ca^{2+} transported from inside to outside of the cells by PCMA and NCX. As a consequence, the cytosolic Ca^{2+} level is down-regulated via promoting the pumping out of intracellular Ca^{2+} , which, in turn, inhibits the influx of extracellular Ca^{2+} . Taken together, these findings indicate that Ca^{2+} homeostasis is essential to maintaining normal corneal repair and that impaired wound healing is able to be treated using a Ca^{2+} chelator such as EDTA, which is able to create a relatively normal cytosolic Ca^{2+} level in the corneal epithelium, or by an inhibitor that blocks downstream of abnormally activated Ca^{2+} signaling, namely is able to block the Ca^{2+} -calcineurin-dependent pathway.

4.6. Transcriptomics of the cornea reveals that *Cisd2* mediates wound healing and maintains epithelial integrity

To understand the molecular mechanism underlying the role of *Cisd2* in corneal wound healing, we perform RNA sequencing using total RNA obtained from the corneas of WT and *Cisd2* KO mice with or without corneal wounding (Fig. 6a). Three sets of pair-wise differential expression genes (DEGs) analyses were performed: (1) between WT and *Cisd2*KO mice with corneal wounding (Set-1); (2) between WT mice with or without corneal wounding (Set-2); (3) between *Cisd2*KO mice with or without corneal wounding (Set-3). In Set-1, the DEGs were defined as genes with a fold change of >1.5 (either up-regulated or down-regulated) and a significance of $p < 0.05$ when WT and *Cisd2*KO are compared. In Set-2 and Set-3, the DEGs were defined as genes with a fold change of >2.0 (either up-regulated or down-regulated) and a significance of $p < 0.01$ compared to their control group.

Interestingly, the level of *Cisd2* mRNA is significantly upregulated in the cornea of WT mice during wound healing (Fig. 6b), which suggests that *Cisd2* plays a role in wound healing. The heatmap reveals that *Cisd2* deficiency affects the expression pattern of a panel of DEGs in the cornea during wounding-induced corneal repair with a total of 315 genes being affected (200 up-regulated and 115 down-regulated genes in *Cisd2*KO mice) (Fig. 6c). These DEGs can be further grouped into a number of different wounding-related pathways. The top six altered pathways are involved in (1) wound healing, stress response, and extracellular matrix; (2) cell cycle, cell death, inflammation, and fibrosis; (3) metabolism; (4) cell differentiation; (5) proteostasis; and (6) cell migration (Fig. 6d). All of these processes and pathways are highly associated with the biology of corneal repair. Furthermore, these results provide molecular insights into the regulation of wounding-induced corneal regeneration and explain the phenotypic defects observed in the *Cisd2*KO mice. Additionally, the unique DEGs in the WT (297 genes; OD wounding vs OS non-wounding) and *Cisd2*KO (304 genes; OD wounding vs OS non-wounding) mice were also analyzed by Gene Ontology annotation (Fig. 6e). Notably, the percentage difference of the wounding-related pathways is

$\mu\text{g}/\text{mL}$), FCCP (1.2 μM), and Rotenone/Antimycin-A (1 μM each) under Seahorse XF24 Extracellular Flux analyzer. (n) Quantification of basal respiration, ATP-coupled respiration, and maximal respiration. (o) Mitochondrial ROS are analyzed by treating cells with 5 μM mitoSOX at 37°C for 30 min. Quantitative analysis is taken under a flow cytometer. (p) Cell proliferation is analyzed for 4 days by the CCK-8 assay. Insert columns indicate the relative cell number at Day 4. (q) HCEC cells (WT, *CISD2*KO and *CISD2*RE) are seeded into silicon inserts with 10% FBS medium. Following cell adhesion, inserts were removed and incubated for 12 h. Quantification of 2D cellular migratory ability is presented as the percentage of wound closure by wound healing assay. (r) HCEC-*CISD2*KO cells are pretreated with Veh or CsA (100 nM) for 30 min before insert removal; 2D cellular migratory ability is quantified after incubation for 12 h. (s) (t) Transwell migration assay of HCEC cells (WT, *CISD2*KO and *CISD2*RE) treated with Veh or CsA (100 nM) for 12 h after seeding. Micrographs for the 0.5% crystal violet staining of migrated cells on the lower surface of the filters are shown(s); magnification 200X. Quantification is presented as percentage of migrated cells compared with WT. (u) (v) Representative picture of IF-stained FAK in HCEC cells (WT, *CISD2*KO and *CISD2*RE). Pseudocolor confocal 2D images and 3D surface plots were taken in the monolayer culture (u) and wound edge (v). (w) Representative picture of IF-stained FAK in HCEC-*CISD2*KO treated with Veh or CsA (100 nM). Pseudocolor confocal 2D images and 3D surface plots were taken in the wound edge. In (b)-(l), the HCEC cells are loaded with 2 μM fura-2/acetoxymethyl ester (fura-2/AM) as fluorescent indicators for cytosolic Ca^{2+} ($[\text{Ca}^{2+}]_i$) at 37°C for 30 min. In (c)-(l), data are represented as mean \pm SEM of at least 100 cells. In (m)-(o), data are represented as mean \pm SD. In (p)-(t), data are represented as mean \pm SEM. All quantitative results are obtained from at least three independent experiments. * $p < 0.05$; ** $p < 0.01$; *** $p < 0.001$. In (c), (e), (g), (i), (n)-(q) and (t), the statistical analysis was performed by one-way ANOVA with Bonferroni multiple comparison test, while in (l) and (r), the statistical analysis was performed by Student's t-test.

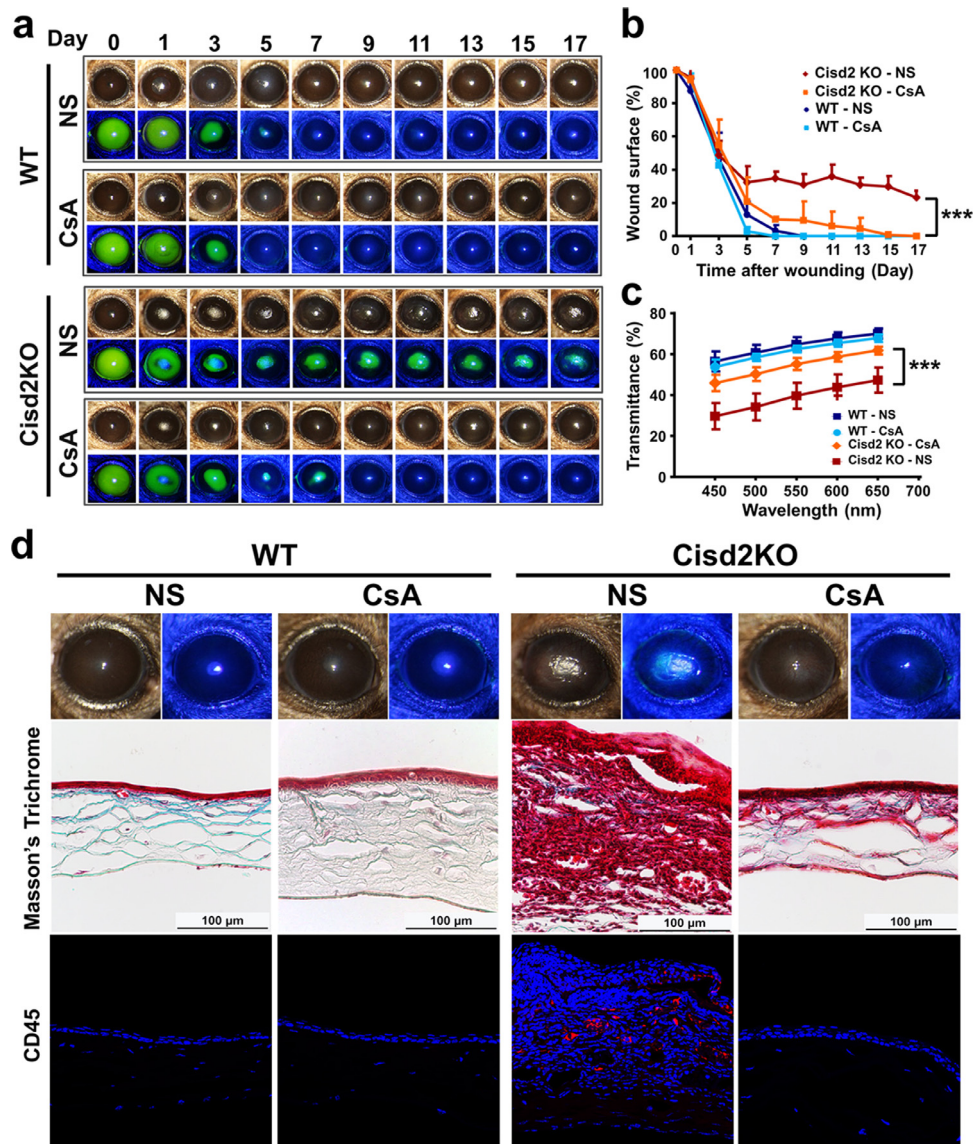


Fig. 5. Cyclosporine A facilitates corneal epithelium wound healing and improves the light transmission of the cornea in Cisd2KO mice. (a) Representative photographs for the corneal wound healing of Cisd2KO and WT mice with cyclosporine A (CsA) or normal saline (NS) treatment. Cisd2KO and WT mice at 3-mo are divided into 4 groups, namely WT-CsA, WT-NS, Cisd2 KO-CsA, and Cisd2KO-NS. A 1.5-mm diameter corneal epithelial defect is made in the right eye using an Alger Brush under anesthesia; the left eye serves as an uninjured control. Cyclosporine A (0.05%) or normal saline (0.9% NaCl) 3 times a day are applied to the injured eyes till the end of the study. In the WT-NS and WT-CsA groups, the corneal wounds are almost completely healed by day 7 after wounding. However, in the Cisd2KO-NS group, delayed wound healing is noted; intriguingly, CsA treatment facilitates the epithelial wound healing in the Cisd2KO-CsA group. (b) Quantification of unhealed wound surface in WT and Cisd2KO mice with CsA or NS treatment (n=3). The injured corneas are stained with 1% fluorescein and photographed with slit lamp every 24 hours for 17 days after the injury, and the size of the unhealed wound surface areas are measured and analyzed by a computer-assisted digitizer (Image J). (c) Quantification of light transmission of the corneas in WT and Cisd2KO mice with CsA or NS treatment (n=3). Light transmission assay is carried out to evaluate the functional improvement by CsA. Immediately after corneal wounding study, the mice were sacrificed and the trephined corneoscleral buttons with endothelial side up are processed for transmission spectrophotometer. The transmittance percentage of the Cisd2 KO-NS group is significantly lower than that in the WT-NS and WT-CsA groups. Remarkably, in the Cisd2 KO-CsA group, the transmittance percentage is significantly higher than that in Cisd2 KO-NS group. Data are presented as mean \pm SD. *** $p < 0.001$. In (b) and (c), the statistical analysis was performed by generalized equation estimation (GEE). (d) Pathological analysis reveals that CsA treatment ameliorates abnormal corneal manifestations and inflammation in the Cisd2KO-CsA group. In both the WT-NS and WT-CsA groups, the corneas remained clear and fluorescein showed negative staining after complete re-epithelialization. In addition, the normal stratification of corneal epithelia and regular alignment of corneal stromal collagen layers are well demonstrated by Masson's trichrome staining; furthermore, CD45-positive cell is not observed in WT cornea. However, in the Cisd2KO-NS group, exaggerated epithelial thickening, abnormal epithelial stratification and loss of stromal collagen rectangular alignment with cellular infiltration were noted. Notably, in the Cisd2KO-CsA group, the abnormal corneal manifestations are ameliorated by CsA treatment; moreover, CD45-positive cell is dramatically diminished after applying CsA.

obviously higher in the Cisd2KO mice compared to the WT mice that have completed corneal repair on day 8 after wounding. In particular, the pathways related to proteostasis and cell migration are present only in the Cisd2KO mice, indicating that Cisd2 deficiency appears to delay corneal wound healing. As a consequence of this, there seems to be a further turning on genes involved in the aging process (Fig. 6f). Collectively, these transcriptomics analyses reveal that Cisd2 plays an essential role in corneal wound healing and this is related to maintaining corneal epithelial integrity.

4.7. Cyclosporine A accelerates corneal repair in patients with epithelial erosion

In humans, it has been reported that topical treatment with 2% CsA, when used as an adjunct therapy, is often able to induce healing of Mooren's ulcers with various degrees of vascularization [34]. However, whether CsA is able to facilitate healing of other human corneal epithelial diseases remains unclear. To explore the therapeutic effect of topical CsA treatment on corneal wound healing, we enrolled five

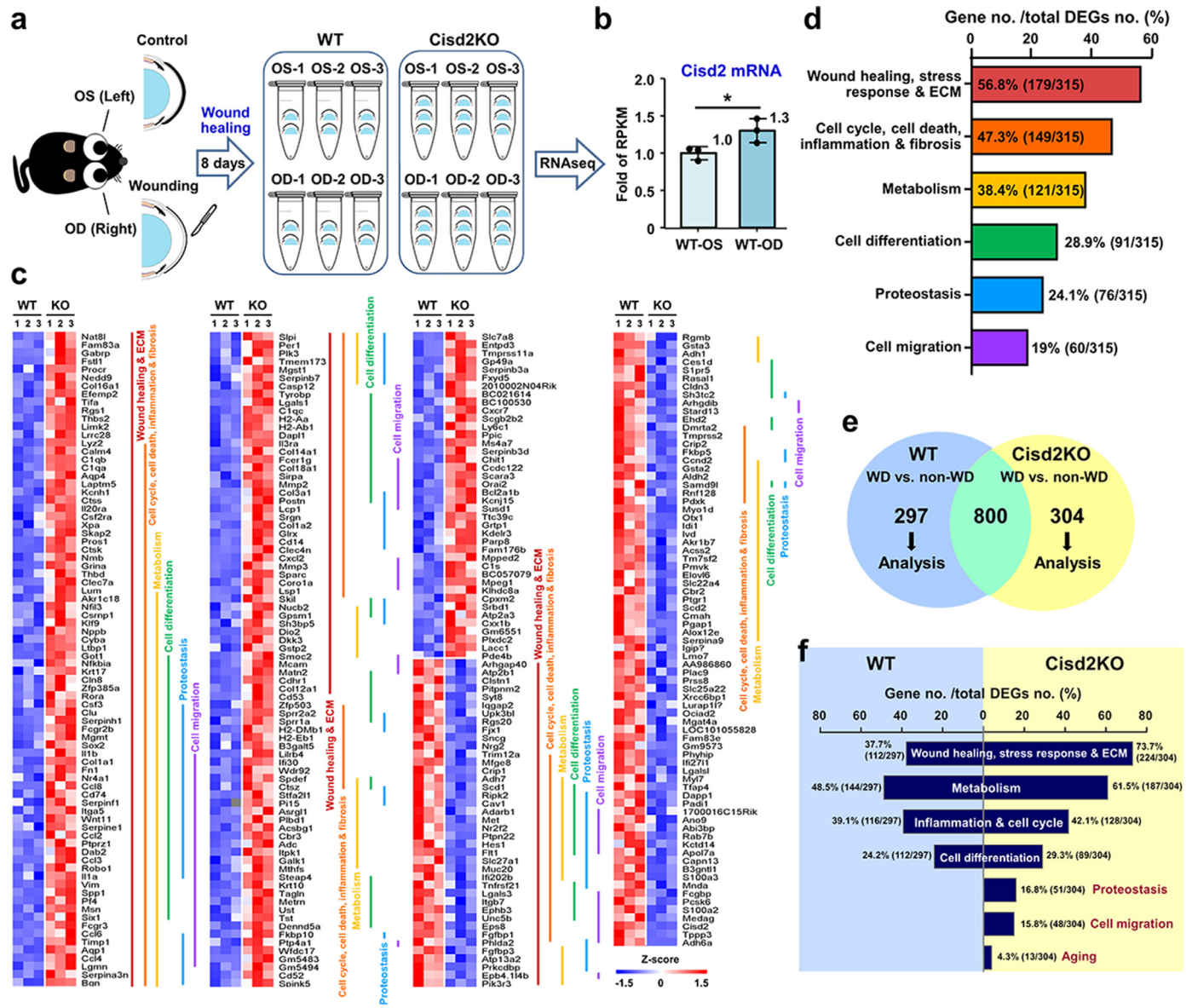


Fig. 6. Corneal transcriptomics reveals that *Cisd2* mediates wounding-induced corneal regeneration in order to maintain corneal epithelial integrity. (a) Collection of corneal tissues from 3-month old WT and *Cisd2*KO mice for transcriptomics analysis. The right eye (OD, oculus dexter) is wounded by cutting into the cornea; the left eye (OS, oculus sinister) is a non-wounded control. The corneal samples are collected at day 8 after wounding. To obtain sufficient amount of RNA for RNA sequencing, we combined two corneal tissues from OS or OD of two mice into one tube in WT mice; while in *Cisd2*KO mice, three corneal tissues from OS or OD of three mice are combined into one tube. (b) The *Cisd2* mRNA levels are up-regulated in the OD (wounded) compared with OS (non-wounded control) in WT mice ($n=3$). Data are presented as mean \pm SD. * $p < 0.05$ by Student's t-test. (c) Heatmap illustrating that *Cisd2* deficiency affects the expression pattern of a panel of DEGs in the cornea after wounding-induced corneal repair. A total of 315 genes are shown (200 up-regulated and 115 down-regulated genes in *Cisd2*KO mice). ECM, extracellular matrix. (d) The DEGs are grouped into different wounding-related pathways and presented by percentage. (e) A Venn diagram illustrating the common and unique DEGs in the WT (OD wounding vs OS non-wounding) and *Cisd2*KO (OD wounding vs OS non-wounding). Numbers represent the amount of significantly changed genes (fold change > 2 , $p < 0.01$) in each pairwise comparison and in their respective overlaps. The unique DEGs in WT (297 genes) and *Cisd2*KO (304 genes) are further analyzed by Gene Ontology annotation. WD, wounding. (f) Percentage difference of the wounding-related pathways between the unique DEGs in WT and *Cisd2*KO mice. In c, d and f, the grouping of pathways is carried out by STRING functional enrichment analysis (Gene Ontology).

patients with moderate to severe dry eye disease; these patients suffered from corneal punctate erosion and refractory symptoms and they had already been treated with standard ocular medications, including artificial tears, topical steroids and 0.05% CsA (Supplementary Table 1). Baseline objective tests, including tear film breakup time (TBUT), corneal fluorescein staining (CFS) scores and external eye photographs were performed. All patients were treated with a higher concentration of CsA (0.1%) for 2 months and then shifted back to 0.05% CsA for another 2 months (Fig. 7a). Interestingly, topical treatment with the higher concentration of CsA (0.1%) resulted in significantly improved TBUT values (Fig. 7b; a longer TBUT means that a more stable pre-corneal tear film is present) and decreased CFS scores (Fig. 7c). These findings not only echo the animal findings

obtained using *Cisd2*KO mice, but also support the use of topical treatment with a higher concentration of CsA in humans, namely 0.1% instead of 0.05%. The latter concentration has been the one normally used clinically for the treatment of corneal epithelial erosions. Our study thus provides evidence indicating that various Ca^{2+} signaling pathways and/or proteins are potential targets for the therapeutic treatment of corneal epithelial diseases in humans.

5. Discussion

Here we provide evidence for the first time to substantiate the hypothesis that *Cisd2* plays an essential role in corneal epithelial integrity and repair, and that *Cisd2* deficiency brings about a vicious

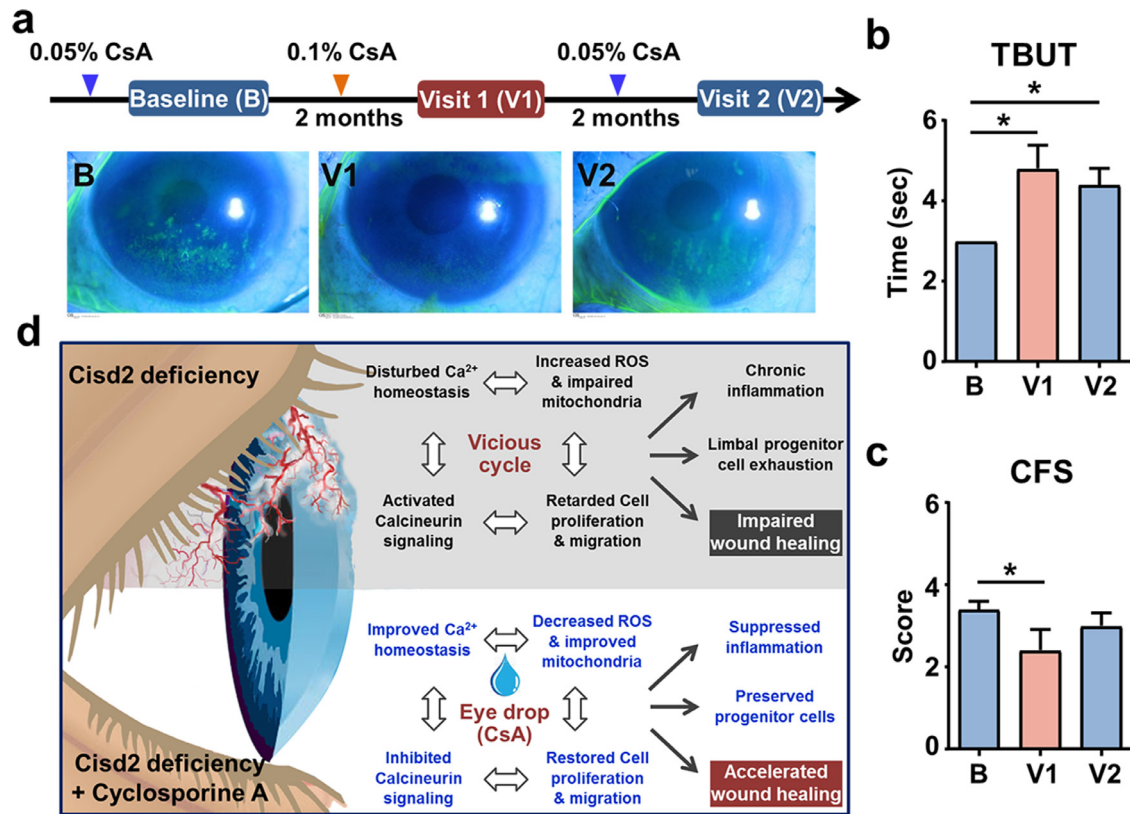


Fig. 7. Cyclosporine A (CsA) repairs corneal epithelial erosion in patients with moderate to severe dry eye diseases. (a) Dry eye patients ($n=5$) who were already under 0.05% CsA twice daily and had been changed to 0.1% CsA once a day due to refractory dry eye symptoms were enrolled in this study. After 2-month treatment with 0.1% CsA, these patients had later shifted back to 0.05% CsA. The time points before 0.05% CsA treatment, two months after 0.1% CsA administration and another two months after shifting back to 0.05% CsA were established as baseline (B), visit 1 (V1) and visit 2 (V2), respectively. Objective parameters including fluorescein tear breakup time (TBUT) and corneal fluorescein staining (CFS) score were used to assess the therapeutic efficacy. A positive green staining of fluorescein indicates the presence of damage to the cornea and this occurs when the dye is able to penetrate the surface. Efficacy analysis was only done in the worst eligible eye, which defined as the higher CFS score at baseline visit. (b) The representative patient shown in (b) is a 69-year old woman with moderate dry eye disease. The CFS score was 4 at baseline in her left eye (left). After 2 months of 0.1% CsA administration, the CFS improved to 2 (middle). And after discontinuation of 0.1% CsA, CFS relapsed to 3 again (right). (c) Efficacy analysis revealed that 0.1% CsA significantly prolonged TBUT in dry eye patients, even after discontinuation of the medication ($p < 0.05$). Moreover, the CFS scores were also significantly improved after treatment with 0.1% CsA. (d) Graphic summary to elaborate the essential role of Cisd2 in corneal epithelial integrity and wound healing. Data are presented as mean \pm SD. * $p < 0.05$ by Student's t-test.

cycle of impaired wound healing that can be treated by cyclosporine A (CsA) (Fig. 7d). Several novel findings are pinpointed in this study. Firstly, in patients with corneal epithelial disease, CISD2 is dramatically down-regulated in their corneal epithelial cells. However, CISD2 continues to be expressed at significant levels in the epithelial layer of ocular diseases that primarily affect the corneal endothelia. Secondly, Cisd2 deficiency in mice causes ocular surface injury and impairs epithelial wound healing, which leads to a chronic damage to the corneal epithelium. This, in turn, activates limbal progenitor cells of mice, which begin to proliferate and differentiate in response to corneal microtrauma; this trauma affects the Cisd2KO cornea continuously and as a consequence, a vicious cycle of persistent corneal injury and repair stimulation ultimately results in the exhaustion of the limbal progenitor cells. Thirdly, mechanistically in human corneal epithelial cells, CISD2 deficiency increases basal cytosolic Ca²⁺ levels, which disturbs intracellular Ca²⁺ homeostasis, impairing mitochondrial function and increasing oxidative stress. These changes hinder cell proliferation and migration, as well as attenuating the dynamic distribution of focal adhesions. The result is retarded corneal regeneration. Furthermore, corneal transcriptomics reveals that Cisd2 in the cornea appears to be involved in wound healing and the maintenance of epithelial integrity. Fourthly, impaired wound healing can be treated, on the one hand, by EDTA, a Ca²⁺ chelator, which is able to reverse the abnormally elevated cytosolic Ca²⁺ and reduce it to a normal level, and, on the other hand, by topical treatment with CsA, an inhibitor of the Ca²⁺-calcineurin-dependent pathway that is activated

by an elevated cytosolic Ca²⁺ level. Intriguingly, in Cisd2KO mice, CsA and EDTA are both able to facilitate epithelial wound healing of the cornea, improve corneal transmittance and suppress inflammatory responses. Finally, and remarkably, topical CsA treatment is able to restore corneal epithelial erosion in patients suffering from moderate to severe dry eye disease. Taking our findings together, this study reveals the translational significance of Cisd2 in corneal epithelial regeneration, and provides evidence that Ca²⁺ signaling pathways are potential targets for the development of therapeutics for corneal epithelial diseases in humans.

5.1. Calcium and corneal wound healing

Maintaining the structural integrity of the corneal epithelium is very important for corneal transparency. Poor epithelial regeneration after injury runs the risk of infection, induces inflammation, and disrupts extracellular matrix remodeling [35]. To achieve successful corneal wound healing, Ca²⁺ mobilization seems to play a pivotal role during epithelial proliferation and migration. Upon injury, extracellular Ca²⁺ influx is necessary to create a large initial Ca²⁺ rise, and to do this intracellular Ca²⁺ stores are released, and this is followed by an intracellular Ca²⁺ wave that spreads from the injured area to the neighboring cells; this wave stimulates cell proliferation and activate the wound healing process [36]. In parallel, there is mobilization of intracellular Ca²⁺ from internal storage via phospholipase C activation and the production of inositol triphosphate (IP3), together with

diacylglycerol (DAG) [37]; this activates downstream signaling including extracellular signal-regulated kinase (ERK), which also promotes corneal epithelial healing [6]. Notwithstanding the above, the temporospatial regulation of the Ca^{2+} response needs to be tightly controlled in order to avoid aberrations in Ca^{2+} signaling that lead to corneal disease [38].

The loss of Ca^{2+} homeostasis found in HCEC-CISD2KO cells results in a significantly elevated level of intracellular Ca^{2+} . As a result, at an early stage, the initial fast Ca^{2+} wave in response to a wound is reduced and the corneal healing process is retarded. However, at a later stage, the elevation in intracellular Ca^{2+} promotes corneal epithelial cells to undergo prematurely terminal differentiation, and this eventually ends up producing a range of corneal phenotypic manifestations. In addition, CISD2KO attenuates the response of HCEC cells to stimulation with capsaicin and histamine; this possibly can be attributed to impaired SOCE activation. However, further study is necessary to identify the mechanisms that underlie the defective SOCE response and the various downstream Ca^{2+} -related signaling pathways.

It seems that there is a discrepancy between the effects of EDTA on the Transwell migration assay of HCEC-CISD2KO cells (Supplementary Fig. 3f) and the corneal wound healing assay of the Cisd2KO mice (Supplementary Fig. 4). In the *in vitro* culture system, EDTA treatment for 12 hr had no beneficial effects on the cell migration ability of the HCEC-CISD2KO cells. One possible explanation is that EDTA treatment for a longer period of time (12 hr) may destroy the interaction between the integrin receptors of cell surface and the extracellular matrix proteins, thereby interfering with the cell migration. However, in the *in vivo* system, under physiological conditions, treatment with EDTA eye drops twice a day was able to significantly improve Cisd2KO mouse corneal wound healing. It seems likely that the repetitively short-term administration of EDTA eye drops on mouse cornea is able to temporarily reduce the intracellular level of Ca^{2+} and thereby promotes corneal wound healing via a suppression of the Ca^{2+} -calcineurin-dependent signaling pathway.

5.2. Focal adhesion dynamics and cell migration

Ca^{2+} signaling is known to regulate focal adhesion dynamics, which is a critical step in the decision process leading to cell migration. The complex process of cell migration includes cytoskeletal organization, actomyosin contraction and focal adhesion turnover. An accumulation of focal adhesions at a peripheral junction enhances the strength of cell connections; however, it also limits the ability to under cell migration as well as its speed. During wound healing, limbal progenitor cells proliferate and migrate toward the front end of the wound edge; when this occurs, formation and aggregation of focal adhesions at the front end of the migrating cells is crucial. Normally in a HECE monolayer, the focal adhesions of the HECE-WT cells are scattered throughout the whole cell. However, we have found that the focal adhesions of HECE-CISD2KO cells gather at the junctions between cells and this may hinder the detachment of cells at the initial stage of migration. At a later stage, the focal adhesions of HECE-WT cells are concentrated at the front end of the wound edge pointing towards the direction of migration. However, in HECE-CISD2KO cells, fewer focal adhesions are found at the leading edge of the migrating cells. Obviously, the defect in the dynamic distribution of focal adhesions found in HECE-CISD2KO cells compromises their migrating ability during wound healing.

Strikingly, CsA treatment of HECE-CISD2KO cells appears to ameliorate the dysregulation of intracellular Ca^{2+} homeostasis; specifically, it reverses the abnormally high levels of basal cytosolic Ca^{2+} and increases the SOCE response. As a consequence, the dynamic distribution of focal adhesions is largely restored, and the migration ability, as measured by 2D and 3D migration assays, is much improved. Taken together, these findings indicate that Ca^{2+} -calcineurin-dependent signaling participates in the phenotypic

manifestations affecting the cornea, and that these abnormalities can be treated by cyclosporine A, which improve wound healing and accelerate corneal repair.

5.3. Cyclosporine A (CsA): beyond anti-inflammation and reaching towards corneal repair

CsA is an immunomodulator that inhibits nuclear factor of activated T cells (NFAT) involved in nuclear translocation. It is on the "World Health Organization model list of essential medicines: 21st list 2019", and is one of the safest and most effective medicines currently used clinically. Most of the pharmacological effects of CsA on the ocular surface are generally believed to be a direct consequence of its ability to inhibit inflammatory T cell infiltration. However, in addition to its anti-inflammatory activity, this study has revealed that (1) CsA promotes epithelial proliferation and cell migration and thus accelerates corneal repair in Cisd2KO mice, and that (2) CsA treatment appears to decrease corneal fluorescein staining scores and seems to facilitate corneal repair in patients with moderate to severe dry eye. Accordingly, these results indicate that, apart from its anti-inflammatory effect, CsA may be used to treat corneal epithelial defects. This new concept has not been proposed in the past except for one report with respect to the treatment of Mooren's ulcers [34]. Nevertheless, there are some important clinical questions that remain unanswered at present. These are: (1) what are the indicated populations of patients; (2) what is the optimal dose of CsA when treating patients; and (3) is possible for CISD2 activators to be applied to promote wound healing of the cornea and/or to protect the cornea from injury.

5.4. Cisd2KO leads to exhaustion of limbal progenitor cells

In general, the cornea is relatively resistant to aging, with almost no or little loss of transparency or other abnormalities occurring among the elderly. A possible explanation for this phenomenon is that corneal epithelial progenitor (stem) cells in the limbus serve as a reservoir for the corneal epithelium. Limbal progenitor cells usually reside in a unique "niche" microenvironment and undergo asymmetric division in response to external insults or injury. Several factors, including cell-cell interactions, interactions between the progenitor cells and the extracellular matrix molecules, cytokines, growth factors, pH and ionic strength (e.g. Ca^{2+} concentration), are important to maintaining this niche microenvironment [39]. It is well known that higher concentrations of extracellular Ca^{2+} induce epithelial cell differentiation [40]. In addition, a previous study has indicated that increasing the Ca^{2+} concentration to 1.2 mM promotes the terminal differentiation of transiently amplifying cells, rather than preserving limbal progenitor cells; this is evidenced by the obvious decline in p63 staining and the clearcut increase in K3/K12 expression [41]. In this study, Cisd2 deficiency causes a sustained elevation of intracellular Ca^{2+} concentration, which results in a vicious cycle of persistent corneal injury and repair stimulation. As a consequence, this leads to the exhaustion of limbal progenitor cells in the cornea of Cisd2KO mice, and ultimately this leads to the development of various ocular manifestations resembling those present in LSCD. Therapies targeting the normalization of Ca^{2+} concentrations, such as eye drops containing cyclosporine A and EDTA, would expect to promote corneal wound healing and the amelioration of any anatomical abnormalities in the cornea. Furthermore, our HCEC-CISD2KO cells may offer a good platform for the development of drugs that target corneal disorders caused by disturbances in Ca^{2+} homeostasis.

5.5. Translational perspectives related to Cisd2 and corneal wound healing

CISD2 is the disease gene involved in Wolfram syndrome type 2 (WFS2, OMIM 604928) and plays a pivotal role in regulating

intracellular Ca^{2+} homeostasis. Wolfram syndrome (WFS; MIM 222300) is a rare autosomal recessive disease that has a wide spectrum of clinical manifestations, including diabetes mellitus (DM), diabetes insipidus, neurosensory deafness, optic atrophy, genitourinary tract disorders and neurological/psychiatric problems [18]. The present study demonstrates that *Cisd2*KO causes Ca^{2+} dysregulation that result in corneal epithelial abnormalities. However, there does not seem to be any previous report describing corneal disorders affecting patients with WFS. One possible explanation is that the lifespan of WFS patients is too short to allow diagnose of these associated corneal diseases [42]. Therefore, based on our findings, it is suggested that the corneal integrity of WFS patients should be evaluated early in their life in order to prevent the development of any visual disabilities associated with *CISD2* deficiency.

5.6. Contributors

CCS co-designed the experiments, conducted/interpreted the results and drafted the manuscript. SYL, LHC, ZQS, CHL and TYT performed the experiments and participated in the data analyses. CHK designed, conducted and interpreted the TEM results. JHSP provided essential research sources. WTC designed, conducted and interpreted the calcium study on HCEC. TFT designed the experiments, analyzed and interpreted the results, and wrote the final manuscript. CCS, WTC and TFT conceived and supervised all experiments and verified the underlying data. All authors read and approved the final version of the manuscript, and ensured it is the case.

Declaration of Competing Interest

None.

Acknowledgments

We thank the Genomics Center for Clinical and Biotechnological Applications of National Core Facility for Biopharmaceuticals, Taiwan (MOST 109-2740-B-010-002) for the RNA sequencing. We thank the technical services provided by the Bioimaging Core Facility of National Core Facility for Biopharmaceuticals, Ministry of Science and Technology, Taiwan. We acknowledge the support provided by grants from the Ministry of Science and Technology (MOST104-2314-B-182-070, MOST105-2314-B-182-066-MY3, and MOST108-2314-B-182-049-MY3 to CCS; MOST 109-2327-B-010-002, MOST 109-2320-B-010-043 and MOST 107-2320-B-010-037-MY3 to TFT), and from Chang Gung Medical Research Foundation (CORPG2L0011 to CCS).

Data Sharing Statement

All data supporting the conclusions of this study are included within the article and its additional files. The data that support the findings of this study are available from the corresponding authors Wen-Tai Chiu and Ting-Fen Tsai upon reasonable request.

Supplementary materials

Supplementary material associated with this article can be found, in the online version, at doi:10.1016/j.ebiom.2021.103654.

References

- [1] Thoft RA, Friend J, The X. Y, Z hypothesis of corneal epithelial maintenance. *Invest Ophthalmol Vis Sci* 1983;24:1442–3.
- [2] Chen HF, Yeung L, Yang KJ, Sun CC. Persistent corneal epithelial defect after pars plana vitrectomy. *Retina* 2016;36:148–55.
- [3] Tsubota K, Goto E, Shimmura S, Shimazaki J. Treatment of persistent corneal epithelial defect by autologous serum application. *Ophthalmology* 1999;106:1984–9.
- [4] Bourne RRA, Flaxman SR, Braithwaite T. Magnitude, temporal trends, and projections of the global prevalence of blindness and distance and near vision impairment: a systematic review and meta-analysis. *Lancet Glob Health* 2017;5:e888–97.
- [5] Liu CY, Kao WWY. Corneal epithelial wound healing. *Prog Mol Biol Transl Sci* 2015;134:61–71.
- [6] Byun YS, Yoo YS, Kwon JY. Diquafosol promotes corneal epithelial healing via intracellular calcium-mediated ERK activation. *Exp Eye Res* 2016;143:89–97.
- [7] Minns MS, Teicher G, Rich CB, Trinkaus-Randall V. Purinoreceptor P2 \times 7 regulation of Ca^{2+} mobilization and cytoskeletal rearrangement is required for corneal reepithelialization after injury. *Am J Pathol* 2016;186:285–96.
- [8] Kawakita T, Espana EM, He H. Calcium-induced abnormal epidermal-like differentiation in cultures of mouse corneal-limbal epithelial cells. *Invest Ophthalmol Vis Sci* 2004;45:3507–12.
- [9] Sun L, Sun TT, Lavker RM. CLED: a calcium-linked protein associated with early epithelial differentiation. *Exp Cell Res* 2000;259:96–106.
- [10] Ma XL, Liu HQ. Effect of calcium on the proliferation and differentiation of murine corneal epithelial cells in vitro. *Int J Ophthalmol* 2011;4:247–9.
- [11] Nagai N, Ogata F, Kawasaki N. Hypercalcemia leads to delayed corneal wound healing in ovariectomized rats. *Biol Pharm Bull* 2015;38:1063–9.
- [12] Najjar DM, Cohen EJ, Rapuano CJ, Laibson PR. EDTA chelation for calcific band keratopathy: results and long-term follow-up. *Am J Ophthalmol* 2004;137:1056–64.
- [13] Al-Hity A, Ramaesh K, Lockington D. EDTA chelation for symptomatic band keratopathy: results and recurrence. *Eye (Lond)* 2018;32:26–31.
- [14] Gimeno FL, Lavigne V, Gatto S. Advances in corneal stem-cell transplantation in rabbits with severe ocular alkali burns. *J Cataract Refract Surg* 2007;33:1958–65.
- [15] Stepp MA, Zieske JD, Trinkaus-Randall V. Wounding the cornea to learn how it heals. *Exp Eye Res* 2014;121:178–93.
- [16] Rouzier C, Moore D, Delorme C. A novel *CISD2* mutation associated with a classical Wolfram syndrome phenotype alters Ca^{2+} homeostasis and ER-mitochondria interactions. *Hum Mol Genet* 2017;26:1599–611.
- [17] Cattaneo M, La Sala L, Rondinelli M. A donor splice site mutation in *CISD2* generates multiple truncated, non-functional isoforms in Wolfram syndrome type 2 patients. *BMC Med Genet* 2017;18:147.
- [18] Khanim F, Kirk J, Latif F, Barrett TG. WFS1/wolframin mutations, Wolfram syndrome, and associated diseases. *Hum Mutat* 2001;17:357–67.
- [19] Chen YF, Kao CH, Chen YT. *Cisd2* deficiency drives premature aging and causes mitochondria-mediated defects in mice. *Genes Dev* 2009;23:1183–94.
- [20] Wu CY, Chen YF, Wang CH. A persistent level of *Cisd2* extends healthy lifespan and delays aging in mice. *Hum Mol Genet* 2012;21:3956–68.
- [21] Wang CH, Chen YF, Wu CY. *Cisd2* modulates the differentiation and functioning of adipocytes by regulating intracellular Ca^{2+} homeostasis. *Hum Mol Genet* 2014;23:4770–85.
- [22] Shen ZQ, Chen YF, Chen JR. *CISD2* haploinsufficiency disrupts calcium homeostasis, causes nonalcoholic fatty liver disease, and promotes hepatocellular carcinoma. *Cell Report* 2017;21:2198–211.
- [23] Yeh CH, Shen ZQ, Hsiung SY. *Cisd2* is essential to delaying cardiac aging and to maintaining heart functions. *PLoS Biol* 2019;17:e3000508.
- [24] Yeh CH, Chou YJ, Kao CH, Tsai TF. Mitochondria and calcium homeostasis: *Cisd2* as a big player in cardiac ageing. *Int J. Mol. Sci.* 2020;21:9238.
- [25] Shen ZQ, Huang YL, Teng YC. *CISD2* maintains cellular homeostasis. *Biochim Biophys Acta Mol Cell Res* 2021;1868:118954.
- [26] Bron AJ, Evans VE, Smith JA. Grading of corneal and conjunctival staining in the context of other dry eye tests. *Cornea* 2003;22:640–50.
- [27] Kao CH, Chen JK, Kuo J, Yang VC. Visualization of the transport pathways of low density lipoproteins across the endothelial cells in the branched regions of rat arteries. *Atherosclerosis* 1995;116:27–41.
- [28] Ran FA, Hsu PD, Lin CY. Double nicking by RNA-guided CRISPR Cas9 for enhanced genome editing specificity. *Cell* 2013;154:1380–9.
- [29] Mi H, Muruganujan A, Ebert D, Huang X, Thomas PD. PANTHER version 14: more genomes, a new PANTHER GO-slim and improvements in enrichment analysis tools. *Nucleic Acids Res* 2019;47:D419–26.
- [30] Szklarczyk D, Gable AL, Lyon D. STRING v11: protein-protein association networks with increased coverage, supporting functional discovery in genome-wide experimental datasets. *Nucleic acids research* 2019;47:D607–D613.
- [31] Howe EA, Sinha R, Schlauch D, Quackenbush J. RNA-Seq analysis in MeV. *Bioinformatics* 2011;27:3209–10.
- [32] Ren H, Wilson G. Apoptosis in the corneal epithelium. *Invest Ophthalmol Vis Sci* 1996;37:1017–25.
- [33] Schermer A, Galvin S, T Sun T. Differentiation-related expression of a major 64K corneal keratin in vivo and in culture suggests limbal location of corneal epithelial stem cells. *J Cell Biol* 1986;103:49–62.
- [34] Tandon R, Chawla B, Verma K. Outcome of treatment of mooren ulcer with topical cyclosporine a 2%. *Cornea* 2008;27:859–61.
- [35] Ueno M, Lyons BL, Burzenski LM. Accelerated wound healing of alkali-burned corneas in MRL mice is associated with a reduced inflammatory signature. *Invest Ophthalmol Vis Sci* 2005;46:4097–106.
- [36] Sung YJ, Sung Z, Ho CL. Intercellular calcium waves mediate preferential cell growth toward the wound edge in polarized hepatic cells. *Exp Cell Res* 2003;287:209–18.
- [37] Neary JT, Kang Y, Bu Y. Mitogenic signaling by ATP/P2Y purinergic receptors in astrocytes: involvement of a calcium dependent protein kinase C, extracellular signal-regulated protein kinase pathway distinct from the phosphatidylinositol-specific phospholipase C/calcium pathway. *J Neurosci* 1999;19:4211–20.
- [38] Berridge MJ, Bootman MD, Roderick HL. Calcium signalling: dynamics, homeostasis and remodelling. *Nat Rev Mol Cell Biol* 2003;4:517–29.

- [39] Jhala D, Vasita R. A review on extracellular matrix mimicking strategies for an artificial stem cell niche. *Polymer Reviews* 2015;55:561–95.
- [40] Kruse FE, Tseng SC. Proliferative and differentiative response of corneal and limbal epithelium to extracellular calcium in serum free clonal cultures. *J Cell Physiol* 1992;151:347–60.
- [41] Meyer-Blazejewska EA, Kruse FE, Bitterer K, Meyer C. Preservation of the limbal stem cell phenotype by appropriate culture techniques. *Invest Ophthalmol Vis Sci* 2010;51:765–74.
- [42] Urano F. Wolfram syndrome: diagnosis, management, and treatment. *Curr Diabetes Rep* 2016;16:6.